Title

Immunolocalisation of aquaporins 3, 7, 9, and 10 in the epididymis of three wild ruminant species (Iberian ibex, mouflon, and chamois) and sperm cryoresistance

Belen Martinez-Madrid[A,*], Carlos Martínez-Cáceres[B], Belén Pequeño[C], Cristina Castaño[C], Adolfo Toledano-Díaz[C], Paula Bóveda[C], Paloma Prieto[D], Manuel Alvarez-Rodriguez[C], Heriberto Rodriguez-Martinez[E], Julián Santiago-Moreno[C]

*Corresponding author:

B Martinez-Madrid

Department of Animal Medicine and Surgery, Faculty of Veterinary Medicine, Complutense University of Madrid, Madrid 28040, Spain.

Email address: belmart@ucm.es

Abstract

Context: In the epididymis, epithelial cells manage changes in the luminal environment for proper sperm maturation. Moreover, aquaglyceroporins modulate epithelial cells' transport of water, glycerol, and other small molecules.

Aims: We aim to characterize the lining epithelium, quantify its cell composition, and immunolocalise AQP3, AQP7, AQP9, and AQP10 alongside the epididymal ductus of three wild ruminant species, and to determine if species-specific differences could be associated with cauda sperm cryoresistance variations.

Methods: Epididymides from Iberian ibex (n=5), mouflon (n=5), and chamois (n=6) were obtained. Cauda spermatozoa were collected, and sperm parameters were analysed before and after freezing. Histology and immunohistochemistry of AQP3, 7, 9, 10, and T-CD3 were performed in the caput, corpus, and cauda epididymal regions.

Key results: This work first describes the lining epithelium in Iberian ibex, mouflon, and chamois epididymis along the three anatomical regions, consisting of principal, basal, apical, clear, and halo cells. However, the percentage of each cell type differed in ibex compared to mouflon and chamois. The positive T-CD3 immunolabeling of all the halo cells confirmed their T-lymphocyte nature. Aquaglyceroporins expression patterns were similar among species, except for differences in AQP7 and AQP10 immunolocalisation in ibex. Species-specific differences in epididymal sperm cryoresistance were confirmed.

Conclusions: The epididymal epithelium of the three wild ruminants differ in their relative number of cell types and AQPs immunolocalization, which ultimately appears to affect cauda epidydimal spermatozoa cryoresistance.

Implications: Our study provides information on the relevance of the epididymal lining epithelium's quantitative composition and AQP pattern expression on sperm cryoresistance.

Keywords: Aquaglyceroporins, chamois, epididymis, epithelial cells, Iberian ibex, immunohistochemistry, mouflon, sperm cryoresistance.

1. INTRODUCTION

Epididymal spermatozoa exhibit a greater cryoresistance than ejaculated spermatozoa in small ruminants, both in domestic (Varisli *et al.* 2009; García-Álvarez *et al.* 2009) and wild species (Martínez-Fresneda *et al.* 2019, 2021). In addition, species-specific differences have been observed in the epidydimal sperm cryoresistance of 19 wild species, including small ruminants (O'Brien *et al.* 2019). Notably, Iberian Ibex (*Capra pyrenaica*), mouflon (*Ovis musimon*), and chamois (*Rupicapra pyrenaica*) showed species-specific differences in sperm cryoresistance in epididymal (Pequeño, Martínez-Madrid *et al.* 2023) and ejaculated spermatozoa (Pradiee *et al.* 2016).

Spermatozoa acquire the ability to become motile and fertilise during their passage through the lengthy, convoluted epididymis duct, where anatomical and physiological regional segments can be drawn. The caput region contributes to water reabsorption and immune system control, and together with the corpus region, to motility acquisition, while the cauda region assures the storage of sperm in a quiescent state thanks to luminal acidification (Nicander 1958; Marengo and Amann 1990; Goyal and Williams 1991; Chen *et al.* 2022). Proper sperm maturation depends on the interaction with the epididymal fluid, a product of secretion and filtration through the pseudostratified lining epithelium. The dynamic changes in the microenvironment composition and concentration along the epididymal lumen are controlled by a well-orchestrated crosstalk between the epithelial cells of the epididymis and between them and the spermatozoa (Cornwall 2009; Chen *et al.* 2022). Thus, species-specific changes in the epididymal fluid microenvironment might affect epididymal sperm resilience to the cryopreservation process.

Epididymal epithelial cells are involved in essential functions for sperm maturation, such as water reabsorption and fluid concentration, protein secretion and clearance, transfer of protein, lipids, and non-coding RNAs to sperm, as well as luminal acidification and immune response that occur in a cell type and region-dependent manner (Ozkocer and Konac 2021; Chen *et al.* 2022). Although the epididymal epithelium has been

characterised in several mammal species, only a few studies have quantified its cell composition along the epididymal regions (Trasler *et al.* 1988; Marengo and Amann 1990; Serre and Robaire 1998; Castro, Gonçalves *et al.* 2017; Menezes *et al.* 2018).

Aquaporins (AQPs) have been postulated as future biomarkers of sperm fertility and freezability (Yeste *et al.* 2017). Among them, the sub-group of aquaglyceroporins, including AQP3, AQP7, AQP9, and AQP10, have a larger pore diameter and lower hydrophilicity than orthodox AQPs, being permeable to water and other molecules, such as glycerol, urea, ammonia, arsenite, hydrogen peroxide, lactate, and acetate (Oberska and Michałek 2021; Delgado-Bermúdez *et al.* 2022). Besides being a metabolic substrate for sperm cells, glycerol is a universal sperm cryoprotectant for most mammals. Interestingly, aquaglyceroporins transport glycerol across the cell membrane with greater preference than water. Thus, establishing "AQPs distribution maps" of the male reproductive tract for each animal species is the initial information for studying AQPs implications in sperm maturation and cryoresistance (Oberska and Michałek 2021).

In this sense, particular variations in the aquaglyceroporin expression and domain location in the spermatozoa appear to be involved in sperm cryoresistance (Yeste *et al.* 2017). Our group has recently immunolocalised AQP3, AQP7, and AQP10 in cauda epididymal and ejaculated spermatozoa of Iberian ibex, mouflon, and chamois (Santiago-Moreno *et al.* 2022; Pequeño, Martínez-Madrid *et al.* 2023), and reported differences in the domain location of AQP10 between cauda epididymal and ejaculated spermatozoa in sheep (Pequeño, Martínez-Madrid *et al.* 2023). Moreover, in ram ejaculates displaying good freezability, the freeze-thawing process increased the proportion of spermatozoa showing AQP3 in the mid and principal pieces (Pequeño, Castaño *et al.* 2023), which could contribute to an increase in the osmo-adaptative capacity of sperm cells (Chen and Duan 2011), pointing AQP3 as a biomarker for sperm cryotolerance in sheep.

In epidydimal epithelial cells, aquaglyceroporins are involved in water absorption to increase sperm concentration and transport and accumulate glycerol and other small molecules necessary for sperm maturation in the epididymal fluid (Cooper and Brooks 1981; Yeste *et al.* 2017; Oberska and Michałek 2021). Moreover, transcriptionally silent epididymal spermatozoa acquire proteins via extracellular vesicles called epididysomes (Sullivan *et al.* 2007). According to Clarke-Bland *et al*. (2022), it is likely to include AQPs among the proteins transferred to maturing spermatozoa via extracellular vesicles. Immunolocalisation of aquaglyceroporins in the epithelial epididymis has already been identified in human (Pastor-Soler *et al.* 2001; Mobasheri *et al.* 2005), rat (Pastor-Soler *et al.* 2001; Badran and Hermo 2002; Hermo *et al.* 2004, 2008; Da Silva *et al.* 2006), buffalo (Arrighi *et al.* 2016), sheep (Schimming *et al.* 2015), horse (Klein *et al.* 2013), pig (Schimming *et al.* 2017), dog (Domeniconi *et al.* 2008; Squillacioti *et al.* 2021), cat (Arrighi and Aralla 2014), two bat species (Oliveira *et al.* 2013; Castro, Kim *et al.* 2017) and two wild rodent species (Menezes *et al.* 2018; Schimming *et al.* 2021). There are still no reports on AQPs immunolocalisation in the epididymis of Iberian ibex, mouflon, and chamois. Unfortunately, even a histological characterisation of the epididymal epithelium is lacking in these species.

Given all the above, we hypothesise that differences in the epithelial cell composition and expression patterns of aquaglyceroporins in Iberian ibex, mouflon, and chamois epididymis could, by modifying the luminal environment where spermatozoa mature, influence their freezability. Therefore, the present study aimed: i) to characterise the lining epithelium of the epididymis in these species and quantify its regional cell composition; ii) to identify the immunolocalisation of AQP3, AQP7, AQP9, and AQP10 alongside the ductus in these species; and iii) to determine if variations in the epididymal epithelium cell composition and AQPs expression patterns among given species could be associated with variations in the cryoresistance of caudal (presumably mature) spermatozoa.

2. METHODS

2.1. Animals and study design

Testes were collected from dead, mature ibexes (n=5), mouflons (n=5), and chamois (n=6) during the rutting season of 2018 (December, October, and October-November, respectively). All animals were legally hunted in their natural habitat by the harvest plans of their specific reserves: for chamois, the Somiedo National Park (43ºN latitude, Province of Asturias, Spain); for ibexes, the Tejeda y Almijara and Serranía de Ronda Game Reserves (36ºN latitude, Malaga, Spain); and for mouflons, the Cazorla and Segura Game Reserve (38ºN, Jaén, Spain). The harvest plans followed the Spanish Harvest Regulation, Forest and Wild Animal Law 8/2003, issued by the corresponding regional governments, which conform to European Union regulations.

The testes were, immediately after being removed from the scrotum, transported to a small laboratory in the game reserve's mountains to reduce sperm and tissue damage. The collected testes were kept at ambient temperature (about 11 ºC) during transport and laboratory processing. Both epididymides were dissected out, and epididymal sperm were immediately collected for later evaluation and cryopreservation. Epididymal regions (caput, corpus, and cauda regions) were visually identified according to previous anatomical descriptions in sheep (Marengo and Amann 1990) and goats (Goyal and Williams 1991), and sections of each region cut by scalpel and fixed in buffered formaldehyde (10 %, pH = 6.9) for at least 48 h.

Study 1. Histological characterisation of the lining epithelium and immunolocalisation of AQP3, AQP7, AQP9, and AQP10 in the Iberian ibex, mouflon, and chamois epididymis

To characterise, quantify and compare the different cell types of the tubular epithelium of the three wild ruminants, a standard hematoxylin and eosin (HE) stain was performed in formalin-fixed and paraffin-embedded sections of the epididymis (caput, corpus, and cauda regions). Additionally, in the same epididymal segments and species,

immunohistochemistry was used to determine and compare between species the immunolocalisation of AQP3, AQP7, AQP9, and AQP10.

Study 2. Epididymal sperm cryoresistance in Iberian ibex, mouflon, and chamois

The quality of spermatozoa retrieved from the cauda region was analysed before and after cryopreservation to investigate differences in epididymal sperm cryoresistance between the three species of wild ruminants.

2.2. Microscopic evaluation and immunohistochemistry staining of the epididymal duct

Samples from the anatomical epididymis (caput, corpus, and cauda regions) were collected, formalin-fixed for at least 48 h, and paraffin-embedded. Three-micrometers-thick section slides were obtained and stained with standard hematoxylin and eosin (H-E) for microscopic evaluation (Feldman and Wolfe 2014). After deparaffination and rehydration, the sections were incubated in Harry´s acidified hematoxylin for 1 min (Thermo Scientific, Madrid, Spain), following a short incubation in alcoholic eosin Y (Thermo) for 30 s. Sections were finally dehydrated, cleared, and mounted with a xylene-based permanent mounting media (Clear Value®, Thermo). The slides were then examined with a direct light conventional microscope (Zeiss Axio Scope AX10, Carl Zeiss, Madrid, Spain) with a high-resolution digital camera (AxioCam 506, Carl Zeiss), and representative images were obtained by using specialised software (Zeiss Zen Lite 3.0, Carl Zeiss). The determination of each cellular type of the tubular epithelium was performed according to Cornwall (2009), establishing epidydimal epithelial cells into principal, apical, basal, clear, and halo cells for each region (caput, corpus, and cauda) and species (Iberian ibex, mouflon, and chamois). Thus, the H-E-stained slides were digitalised using a high-resolution digital slide scanner (Pannoramic MIDI-II, 3D Histech, Budapest, Hungary). The scanned sections were digitally examined with special

software (Slide Viewer, Ver. 2.5, 3D Histech). A minimum of five random whole tubules of each region (in a transversal plane) were examined at 400X, classifying the cells according to their histomorphologic features. The percentage of each cell type was finally calculated based on the total epithelial cell number of the tubule.

To determine the immunohistochemical distribution of AQP3, AQP7, AQP9, and AQP10, indirect ABC procedures were carried out in serial 3 µm-thick epididymis sections (Hsu and Raine 1981). Briefly, after deparaffination and rehydration, a heat-induced demasking antigen retrieval procedure was performed using a commercial target retrieval solution (EDTA pH 9, Agilent Dako, Madrid, Spain) for 30 min at 97 ºC. Endogenous peroxidase was then blocked with a commercial solution (Agilent-Dako) for 5 min at room temperature (RT), followed by incubation with normal horse serum (30 min at 37 ºC, Vector Labs., Barcelona, Spain) to block unspecific immunolabeling. After these procedures, the sections were overnight incubated at 4 ºC with primary antibodies at their respective dilution (rabbit anti-human AQP3 (ref. AQP003, dilution 1/300, Alomone Labs., Jerusalem, Israel), rabbit anti-human AQP7 (ref. AQP007, dilution 1/250, Alomone), rabbit anti-human AQP9 (ref. AQP009, dilution 1/250, Alomone), and rabbit anti-human AQP10 (ref. ab81179, dilution 1/100, Abcam B.V., Netherlands). The following day, the sections were incubated with a secondary anti-rabbit HRP-labeled polymer (ImPress, Vector Labs, Burlingame, USA) for 30 min at 37 ºC. The positive immunoreaction was revealed by incubating the sections with a commercial 3diaminobenzidinedine solution (DAB) for 5 min at RT (Agilent Dako). Sections were additionally hematoxylin counterstained, dehydrated, cleared, and mounted in a permanent mounting media (HistoMount, Merck, Madrid, Spain). A dark brown precipitated with a membrane-stain pattern identified positive immunoreaction. Positive and negative controls were included to establish the accuracy of the immunolabeling. Positive control immunolabeling consisted of mouse kidney (for AQP3), rat kidney (for AQP7), rat liver (for AQP9), and human yeyune (for AQP10), according to previously

published studies (Li *et al.* 2005; Nilsson *et al.* 2012; Chung *et al.* 2019; Cheng *et al.* 2021) and recommended by the manufacturers (Fig. S1). The same immunohistochemical procedure was carried out for negative controls on sections of all epididymal tissues, omitting the primary antibody incubation step (Fig. S2). Additionally, ovine kidney was included to test AQP3, AQP7, and AQP9 immunolabeling in ruminant tissues (Fig S3). To test the specificity of positive immunolabelling, the same immunohistochemical procedure was simultaneously performed in caput, corpus, and cauda epididymal tissue of ibex, mouflon, and chamois by applying a specific blocking peptide for AQP3 (ref. BLP-QP003, dilution 1/300, Alomone), AQP7 (ref. BLP-QP007, dilution 1/250, Alomone), and AQP9 (ref. BLP-QP009, dilution 1/250, Alomone), according with manufacturer´s specifications (Fig S3). The absence of positive immunolabeling was established as a presumable specificity of the antibody. AQP10-blocking peptide was not available by Abcam, and thus, the specificity of the AQP10 antibody could not be assessed by peptide competition assay.

Lastly, to characterise the immunophenotype of the intraepithelial round cells, previously classified as halo cells, an indirect ABC procedure was also performed by using a rabbit anti-human CD3 antigen (ref. A452, dilution 1/500, Agilent Dako,) following the same procedure described above. Like AQP expression, a dark brown precipitated with a membrane-stain pattern identified positive immunoreaction.

2.3. Epididymal sperm collection, cryopreservation, and evaluation

Epididymal spermatozoa were collected from the cauda region between 4-9 h after death for ibexes and mouflons and 9-18 h after death for chamois by the retrograde flushing method at ambient temperature (11 ºC–13 ºC in the field laboratory) (Santiago-Moreno *et al.* 2009).

The semen extender used to flush and extend the spermatozoa varied according to species. For chamois and ibex sperm collection, 1 ml of a Tris-citric acid-glucose-based (TCG) extender composed of Tris (313.7 mM), citric acid (104.7 mM), glucose (30.3 mM), 6 % egg yolk (vol/vol) was used. In comparison, mouflon spermatozoa were collected using 1 ml of a Tris-TES-glucose-based (TTG) extender composed of Tris (95.8 mM), TES (210.6 mM), glucose (10.1 mM), and 6 % egg yolk (vol/vol), 320 mOsm/kg. Both were prepared using reagent-grade chemicals purchased from Panreac Química S.A. (Barcelona, Spain) and Sigma Chemical Co. (St. Louis, Missouri, USA). The osmolarity of each extender was 345 mOsm/kg for TCG and 320 mOsm/kg for TTG. Extenders were adjusted to pH 6.8.

Epididymal sperm samples were extended in TCG or TTG extender, depending on the species, to a final concentration of 800×10^6 sperm/mL. The samples were cooled at 5 °C for one hour. Glycerol was added to a final concentration of 5 % (v:v), and after 15 min of equilibration at 5 ºC, the samples were loaded into 0.25 mL straws and frozen by placing them in the nitrogen vapor 5 cm above the surface of a liquid nitrogen bath, for 10 min before plunging them into the liquid nitrogen (Pradiee *et al.* 2016).

After sperm collection, concentration was measured in the samples with 1 mL of extender after flushing, using a Neubauer chamber (Marienfeld, Lauda-Königshofen, Germany). The percentage of motile spermatozoa and the quality of sperm motility, determined by the vigor of spermatozoa movement scored on a scale from 0 (lowest) to 5 (highest), were evaluated using a phase-contrast microscope (Zeiss, Germany) at 100x (samples were previously incubated for 5 min at 37 ºC). Proportions of viable spermatozoa were assessed using a nigrosin-eosin (NE) stain (Campbell *et al.* 1956), while sperm membrane functional integrity was determined (%) by the hypoosmotic swelling test (HOST) (Jeyendran *et al.* 1984). Morphological abnormalities and the proportion of spermatozoa showing an intact acrosome apical ridge were assessed in samples fixed in buffered 2% glutaraldehyde solution at 37 ºC, using phase-contrast

252 microscopy (magnification 1000×) (counting 200 cells) (Pursel and Johnson 1974). The
253 apical/distal cytoplasmic droplet was not considered a morphological abnormality in
254 epididymal samples.

255 After 1 to 2 years, frozen samples were thawed by placing the straws in a water
256 bath at 37 ºC for 30 seconds, emptying the content into 1.5 mL Eppendorf
257 microcentrifuge tubes (Eppendorf Iberica SLU, Madrid, Spain) and incubating it for 5 min
258 at the same temperature. Plasma membrane functional integrity, acrosome ridge
259 integrity, sperm viability, and morphological abnormalities were assessed in frozen-
260 thawed samples in the same way as for fresh spermatozoa. In addition, sperm motility
261 and kinetic sperm parameters were evaluated with a computer-aided sperm analyses
262 (CASA) system (SCA®, Microptic S.L., Barcelona, Spain) coupled with a phase contrast
263 microscope (Nikon Eclipse 50i; negative contrast, Tokyo, Japan) and a camera (A312fc;
264 Basler AG, Ahrensburg, Germany), which were not available for use in fresh samples in
265 the field. For this, sperm samples were -for better visualisation- extended (1:80, v:v) with
266 the TCG or TTG extender, respectively, and three µL drops were placed on a Leja eight-
267 chamber slide (Leja Products B.V., Nieuw Vennep, The Netherlands). All materials were
268 tempered at 37 º C. A minimum of three fields and 500 sperm cells were examined per
269 sample with the 10X objective (images acquisition rate 50 frames/s) with settings
270 adjusted for Iberian ibex, mouflon, and chamois spermatozoa. The following parameters
271 were assessed: total sperm motility (TM; %), progressive sperm motility (PM; %),
272 curvilinear velocity (VCL; mm/s), straight-line velocity (VSL; mm/s), the average path
273 velocity (VAP; mm/s), and the amplitude of lateral head displacement (ALH; mm). Total
274 motility included all spermatozoa in motion, regardless of the type of movement, whereas
275 progressive motility was considered when STR>80 %.
276

277 *2.4. Statistical analyses*

All calculations were performed using STATISTICA software for Windows v.12.0 (StatSoft Inc., Tulsa, OK, USA). In addition, epithelial cell types were also analysed using the PRISM software for Windows Version 8.0.2 (263) (GraftPad Soft, Inc.). Data were expressed as means ± standard error of the mean (SEM). The sperm variables were not normally distributed as determined by Shapiro–Wilk test, even after arcsine transformations. Therefore, the nonparametric Mann-Whitney U-test for unmatched samples was used to compare differences between species. The homogeneity of variance was assessed using the Levene test. The proportion of epithelial cell types on epididymal caput, corpus, and cauda regions of ibex, mouflon, and chamois was analysed by one way-ANOVA. When values were not normally distributed as determined by Shapiro–Wilk test, the nonparametric Kruskal–Wallis analysis was used. Where applicable, significance was set at $P<0.05$.

3. RESULTS

Study 1. Histological characterisation of the lining epithelium and immunolocalisation of AQP3, AQP7, AQP9, and AQP10 in the Iberian ibex, mouflon, and chamois epididymis

Representative images of the anatomical caput, corpus, and cauda regions of the Iberian ibex, mouflon, and chamois epididymis are shown in Figs. 1 to 3. The epididymis consists of a highly tortuous tubule lined by epithelial cells, conforming a pseudostratified epithelium of several cell types, including principal, basal, apical, clear, and halo cells, surrounded by a lamina propia developed beyond the peritubular muscle layer, forming the periductal stroma. In the three species, all the epithelial cell types were observed in all the epididymal regions (caput, corpus, and cauda) (Figs. 1–3). According to species and regions, principal cells were the primary cell type, varying from 61.5 ± 1.4 % to 88.0 ± 2.3 % (Table 1). These cells were columnar, clearly visible from the lumen to the basement of the tubule, with an oval heterochromatic nucleus located in the basal or lower third of the cell and well-defined stereocilia on the luminal side. Basal cells were the second more frequent cell type observed (from 6.2 ± 0.4 % to 28.1 ± 1.2 %, depending on species and regions). These round-shaped cells, with basal location, present an elliptical euchromatic nucleus with a prominent nucleolus. Apical cells display morphologic features to principal cells, but this subpopulation is located near the tubule's luminal side and does not contact the basement. On the other hand, clear cells are a subpopulation characterised by numerous acidophilic vesicles in the apical region, which displace the nucleus to the basement. Lastly, halo cells are small, round-shaped cells, usually located in the basement, with a small oval heterochromatic nucleus surrounded by a narrow rim of clear cytoplasm. We could clearly identify all the halo cells by the positive immunolabeling to the T-CD3 antigen (a typical marker for T-lymphocytes) of these cells in all epididymal regions from the three species (Fig. 4).

The percentage of the epithelial cell types varied (P<0.05) according to species (Fig. 5) and epididymal regions (Table 1). Regarding species, Iberian ibex presented a

lower (P<0.0001) percentage of principal cells and a higher (P<0.0001) percentage of basal cells than mouflon and chamois, as well as a higher (P<0.005) percentage of clear and halo cells than mouflon (Fig. 5). On the other hand, considering the epididymal region, differences between species (P<0.05) were found in the percentage of principal, basal, apical, and clear cells but not in halo cells (Table 1)

Regarding AQPs expression, positive (Fig. S1) and negative (Fig. S2) controls were immunostained to ensure the antibody's specificity and the lack of background induced by the secondary antibody, respectively. For positive controls, positive immunostaining was also identified as membrane-pattern labeling. The specificity of AQP3, AQP7, and AQP9 antibodies was successfully proved by peptide-blocking experiments in the caput, corpus, and cauda epididymis of ibex, mouflon, and chamois (illustrative images are shown in Fig. S3).

The main expression membrane patterns of the studied AQPs in the epithelial cells of the different epididymal regions of the three species are summarised in Table 2. Regarding the caput region, AQP3-positive immunostaining was observed in the membrane of sporadic basal cells in all species (Fig. 6*a*–*c*). A weak membrane-pattern immunolabeling to AQP7 was observed in principal cells in all species (Fig. 6*d*–*f*), whereas only in basal cells of Iberian ibex (Fig. 6*d*) and apical cells of mouflon and chamois ducts (Fig. 6*e, f*). A common expression pattern was observed in AQP9 both in apical (principal and apical cells) and basal (principal and basal cells) membranes in all species (Fig. 6*g*–*i*). Lastly, no AQP10 immunostaining was observed in any duct from the caput of the three species (Fig. 6*j*–*l*).

In the corpus region, AQP3-positive immunostaining was observed in all species' apical membranes of principal and apical cells (Fig. 7*a*–*c*). A weak immunolabeling to AQP7 was observed in basal cells in the three species (Fig. 7*d*–*f*). The expression pattern of AQP9 (Fig. 7*g*–*i*) was identical to that observed in the caput region. Whereas no immunostaining for AQP10 was observed in ibex (Fig. 7*j*), mouflon and chamois ducts

showed positive AQP10 immunolabeling both in principal and apical (apical membrane) and basal cells (Fig. 7*k, l*).

In the cauda region, the AQP3 expression pattern (Fig. 8*a*–*c*) was identical to that observed in the caput region. AQP7 positive immunostaining was observed in the apical membrane of principal cells in ibex ducts (Fig. 8*d*), scattered principal cells in mouflon (Fig. 8*e*), and no labeling was found in chamois (Fig. 8*f*). The AQP9 expression pattern was the same as in the caput and corpus region, except for the lack of labeling in basal cells and basal membrane of principal cells. (Fig. 8*g*–*i*). Lastly, positive immunostaining for AQP10 was observed in principal (apical membrane) and basal cells in ibex (Fig. 8*j*), whereas in mouflon and chamois was restricted to basal cells (Fig. 8*k, l*). A detail of the AQPs positive immunolabeling on the different epithelial cell types of the ibex, mouflon, and chamois epididymis are provided as supplementary figures for the caput (Fig. S4), corpus (Fig. S5), and cauda regions (Fig. S6).

The apical blebs of the epithelial cells of Iberian ibex, mouflon, and chamois epididymis showed positive AQP3, 7, 9, and 10 immunostaining, except in the caput region of ibex and mouflon for AQP3, and the cauda region of the three species for AQP3 and AQP10 (Table S1). Illustrative images of the apical blebs immunolabeling are provided as supplementary figure (Fig. S7).

Study 2. Epididymal sperm cryoresistance in Iberian ibex, mouflon, and chamois

In fresh samples of caudal contents, sperm concentration, quality of motility, and membrane functional integrity were influenced by species (Table 3). Mouflon spermatozoa showed significantly higher ($P<0.05$) concentration than ibex and chamois and higher ($P<0.05$) quality of motility than chamois. In contrast, sperm membrane functional integrity was higher ($P<0.05$) in ibex than in chamois.

In frozen-thawed samples, sperm viability, membrane functional integrity, and some kinetic parameters were influenced by species (Table 3). Chamois spermatozoa showed significantly higher (P<0.05) viability after thawing than mouflon, whereas sperm functional integrity was better preserved (P<0.05) in ibex compared to mouflon. Mouflon presented higher (P<0.05) curvilinear velocity (VCL) than chamois and higher (P<0.05) straight-line velocity (VSL) and average path velocity (VAP) than the other two species. Ibex VSL and VAP were also higher (P<0.05) than in chamois.

4. DISCUSSION

The present work has characterised, for the first time, the epididymal epithelium and the expression patterns of aquaglyceroporins in Iberian ibex, mouflon, and chamois. The epithelium of the three species included the same cell types (principal, basal, apical, clear, and halo cells) in all the epididymal anatomical regions. Still, ibex showed differences in the relative percentage of each one compared to mouflon and chamois. Moreover, the three species' epididymal epithelium had positive immunolabeling to AQP3, AQP7, AQP9, and AQP10 in a cell membrane location, with similar patterns, except for some differences in the immunolocalisation of AQP7 and AQP10 in ibex. Data also confirmed species-specific differences in cauda epididymal sperm cryoresistance.

Principal cells were the most abundant (from 61,1 % to 88 % of the total epithelial cells, depending on species and region), followed by basal cells, in agreement with previous reports in sheep (Marengo and Amann 1990), rat (Trasler *et al.* 1988; Serre and Robaire 1998), black-footed colilargo (*Oligoryzomys nigripes*) (Menezes *et al.* 2018) and common bat (*Desmodus rotundus*) (Castro, Gonçalves *et al.* 2017). The comparison among species revealed quantitative but not qualitative differences. Ibex presented the lowest percentage of principal cells, the highest rate of basal cells, and a higher percentage of clear and halo cells than mouflon. The expression patterns of AQP3 and AQP9 in the epididymal epithelial cells were identical for the three wild ungulates. However, Ibex varied in the immunolocalisation of AQP7 in caput and cauda regions and AQP10 in corpus and cauda epididymis, compared to mouflon and chamois. Thus, in our study, the differences in the relative number of each epithelial cell type along the epididymis and aquaglyceroporins immunolocalisation could partially explain changes in the environment where sperm maturation occurred, which could influence the higher sperm resistance to osmotic stress in ibex or the better sperm motility in mouflon.

Epithelial cells prevent autoimmune responses against auto-antigenic spermatozoa while protecting against ascending and blood pathogens. Halo cells have

403 traditionally been considered intraepithelial leukocytes (Flickinger *et al.* 1997; Serre and
404 Robaire 1999; Robaire and Hinton 2015). Our results confirmed the T-lymphocyte nature
405 of all the halo cells in ibex, mouflon, and chamois. Moreover, while principal cells form
406 the blood–epididymal barrier (Cornwall 2009), clear cells respond to inflammatory
407 conditions or bacterial antigens (Battistone *et al.* 2019), and basal cells detoxify factors
408 from blood or principal cells (Chen *et al.* 2022), suggesting a clear physiological interplay
409 for the constituent cell types.

410 AQP9 plays an essential role in intraluminal fluid secretion and reabsorption
411 dynamics of the epididymis. AQP9 is the most abundant aquaglyceroporin isoform in the
412 epididymis; it has been reported in human (Pastor-Soler *et al.* 2001), rat (Pastor-Soler *et*
413 *al.* 2001; Badran and Hermo 2002; Da Silva *et al.* 2006; Hermo *et al.* 2008), horse (Klein
414 *et al.* 2013), buffalo (Arrighi *et al.* 2016), sheep (Schimming *et al.* 2015), pig (Schimming
415 *et al.* 2017), dog (Squillacioti *et al.* 2021), cat (Arrighi and Aralla 2014), common vampire
416 (*Desmodus rotundus*) (Castro, Kim *et al.* 2017), great fruit-eating bat (*Artibeus lituratus*)
417 (Oliveira *et al.* 2013), Azaras'agouti (*Dasyprocta azarae*) (Schimming *et al.* 2021), and
418 black-footed colilargo (*Oligoryzomys nigripes*) (Menezes *et al.* 2018).

419 Ibex, mouflon, and chamois epididymides showed positive AQP9 immunostaining
420 in principal, apical, and basal cells in caput and corpus regions and principal and apical
421 cells in the cauda region. Sheep (Schimming *et al.* 2015) and Azara's agouti (Schimming
422 *et al.* 2021) showed a similar AQP9 expression pattern but in a nuclear location instead
423 of the membrane location of the three wild ungulates. However, in ram cauda epididymis,
424 the apical epithelial lining, including microvilli, was also positive for AQP9. The other
425 reported species expressed AQP9 only in the principal cells along the epididymis,
426 varying in the cell location (membrane, nucleus, or cytoplasmic) and immunoreaction
427 intensity. Sporadic clear cells had positive immunolabeling to AQP9 in the rat corpus
428 (Hermo *et al.* 2008) and cauda (Badran and Hermo 2002; Hermo *et al.* 2008), and
429 sporadic basal cells in the dog cauda epididymis (Squillacioti *et al.* 2021). Moreover, in

buffalo, principal cells did not immunostain for AQP9 in the caput epididymis, and the expression pattern in corpus and cauda varied depending on the season and the animal age (Arrighi *et al.* 2016).

Along with AQP9, the presence of AQP3 and AQP7 in the epididymis of some species suggests their role in the luminal transport of water, glycerol, and other solutes for sperm maturation (Yeste *et al.* 2017; Oberska and Michałek 2021). However, the immunolocalisation of AQP3 in the epididymis has only been reported in the human (Mobasheri *et al.* 2005), in ciliated epithelial cells, and the rat (Hermo *et al.* 2004), in basal cells; and the immunolocalisation of AQP7 in the rat (Hermo *et al.* 2008), in principal cells along the epididymis and some clear cells in the corpus, and the dog, in principal cells of the caput (Domeniconi *et al.* 2008; Squillacioti *et al.* 2021) and cauda region (Squillacioti *et al.* 2021) and basal and some clear cells in the corpus region (Squillacioti *et al.* 2021). In the horse, AQP3 and AQP7 transcripts were found in all the epididymal regions, but no IHC was performed to identify if epithelial cells expressed them (Klein *et al.* 2013).

The AQP3 expression pattern in ibex, mouflon, and chamois was similar to the rat (Hermo *et al.* 2004) in caput and cauda regions, where sporadic basal cells were positive, but not in the corpus region, where principal and apical cells but not basal cells were positive. Moreover, our results confirmed the species-specificity expression pattern of AQP7: in the caput epididymis, principal cells had positive immunolabeling to AQP7 in the three wild ruminants, similar to the rat (Hermo *et al.* 2008) and dog (Domeniconi *et al.* 2008; Squillacioti *et al.* 2021), but differently, basal cells were also positive in ibex and sporadic apical cells in mouflon and chamois; in the corpus region, basal cells were positive in ibex, mouflon, and chamois, identical to the dog (Squillacioti *et al.* 2021) but different to the rat (Hermo *et al.* 2008); and in the cauda region, the immunolocalisation was similar for ibex, mouflon, rats (Hermo *et al.* 2008) and dog (Squillacioti *et al.* 2021), while chamois was not positive for AQP7 immunostaining in principal cells.

457 The role of AQP10 in the epididymis is less known. Indeed, this is the first report
458 of AQP10 immunolocalisation in epididymal epithelial cells. In rat epididymis, only
459 endothelial but not epithelial cells had positive immunostaining of AQP10 (Hermo *et al.*
460 2004). Finally, AQP10 transcripts were found in all the epididymal regions in the horse,
461 but differently from AQP3 and AQP7, with lower immunolabeling in epididymis than in
462 the testis, suggesting a less relevant role in these tissues (Klein *et al.* 2013).

463 Species-specific differences in the epididymal epithelium and the AQP7 and
464 AQP10 expression patterns might affect the epididymal fluid microenvironment. This fact
465 could produce changes in epididymal sperm sensitivity to the cryopreservation process.
466 In fact, cauda epididymal spermatozoa of Iberian ibex showed the highest values for
467 sperm membrane functional integrity (HOST) and mouflon for some sperm kinetic
468 parameters, both fresh and after thawing. Similarly, Pequeño *et al*. (Pequeño, Martínez-
469 Madrid *et al.* 2023) reported a higher HOST cryoresistance ratio in the ibex cauda
470 epididymal sperm than in chamois and mouflon. Differences in sperm head dimension
471 (O'Brien *et al.* 2019), lipid composition (Mocé *et al.* 2010), proteome (Martínez-Fresneda
472 *et al.* 2021), and AQP expression and domain location (Yeste *et al.* 2017) could partially
473 explain sperm freezability variations among species. However, the epididymal epithelium
474 composition is an unexplored factor for sperm cryoresistance underlying mechanisms.

475 Along the epididymis, the epithelial cells are responsible for water reabsorption,
476 luminal acidification, transfer of proteins, lipids, RNA, and non-coding RNAs to sperm,
477 and the immune response, in a cell-type dependent manner (Ozkocer and Konac 2021).
478 Moreover, a given cell type could play different roles depending on the epididymal region,
479 neighboring cell communication, and other stimuli (Battistone *et al.* 2019). In addition,
480 the expression of aquaglyceroporins in the epithelial cells modulates water, glycerol, and
481 other solutes transport across membranes, which also modifies the osmolarity and
482 composition of the epididymal fluid (Yeste *et al.* 2017; Oberska and Michałek 2021).

Finally, the positive immunolabeling of AQPs in the apical blebs of the epithelial cells may support the hypothesis of the AQP acquisition by epididymal spermatozoa via epididysomes derived from these blebs. Epididysomes are released to the lumen by an apocrine mechanism that involves the formation of apical blebs in the principal (Ozkocer and Konac 2021) and clear cells (Barrachina *et al.* 2022) and their further detachment from the apical membrane, liberating their content, which includes these small membrane vesicles (Sullivan *et al.* 2007). Moreover, most AQPs, specifically AQP1, 2, 3, 4, 5, 7, and 9, have been identified in extracellular vesicles of various species and cell types (Clarke-Bland *et al.* 2022). However, AQPs have not yet been identified in extracellular vesicles derived from the mammalian male reproductive system (Candenas and Chianese 2020). So, further studies are needed to elucidate if AQPs are among the proteins transferred to maturing spermatozoa via epididysomes.

5. CONCLUSIONS

Iberian ibex, mouflon, and chamois showed differences in their epididymal epithelium, particularly in the relative number of each epithelial cell type and the immunolocalisation of AQP7 and AQP10, which, together, could contribute to modifying the environment during sperm maturation and, thus, the cryoresistance of caudal spermatozoa.

Data Availability.

The data supporting this study's findings are available from the corresponding author upon reasonable request.

Conflicts of interest.

The authors declare no conflicts of interest.

Declaration of funding.

This study was supported by PID2020-113288RB-100 / AEI / 10.13039/501100011033. In addition, B. Pequeño received a grant for pre-doctoral researchers from AEI (PRE2018-085637)

Acknowledgements.

The authors thank the *Ayuntamiento de Sedella* (Málaga, Spain) for providing field laboratory facilities in the Tejeda y Almijara Game Reserve, the *Parque Natural Sierras de Cazorla, Segura y las Villas*, and the *Consejería de Sostenibilidad, Medio Ambiente y Economía Azul, Junta de Andalucía*, for their unfailing help in the provision of biological samples and in implementing the projects proposed.

Author affiliations.

[A] Department of Animal Medicine and Surgery, Faculty of Veterinary Medicine, Complutense University of Madrid, Madrid 28040, Spain.

[B] Investigation Support Platforms, Biomedical Research Institute of Murcia-Virgen de la Arrixaca (IMIB-Arrixaca), Murcia, Spain. IMIB. Ctra. Buenavista s/n, 30120. El Palmar, Murcia, Spain.

[C] Department of Animal Reproduction, National Institute for Agricultural and Food Research and Technology, Spanish Scientific Research Council (INIA-CSIC), Avda. Puerta de Hierro km 5.9, 28040 Madrid, Spain.

[D] Consejería de Sostenibilidad, Medio Ambiente y Economía Azul, Junta de Andalucía, Jaén, Spain.

[E] Department of Biomedical and Clinical Sciences (BKV), Obstetrics and Gynecology, Linköping University, Linköping, Sweden.

AUTHOR CONTRIBUTIONS

B. Martinez-Madrid: Data adquisition, data analysis/interpretation, manuscript drafting, investigation, critical revision of the manuscript and editing, approval of the article. **C. Martinez-Cáceres**: Data acquisition, data analysis/interpretation, investigation, methodology, resources, critical revision of the manuscript, and editing. **B. Pequeño:** Acquisition of data, data analysis/interpretation, investigation. **C Castaño:** Data analysis/interpretation, methodology. **A. Toledano-Díaz:** Data analysis/interpretation, methodology. **P. Bóveda:** Data analysis/interpretation, methodology. **P. Prieto:** Data analysis/interpretation, resources. **M. Alvarez-Rodriguez:** Data analysis/interpretation, investigation. **H. Rodriguez-Martinez:** Concept/design, investigation, critical manuscript revision, and editing. **J. Santiago-Moreno:** Concept/design, data analysis/interpretation, investigation, critical manuscript revision and editing, funding acquisition, article approval.

REFERENCES

Arrighi S., and Aralla M. (2014). Immunolocalization of Aquaporin Water Channels in the Domestic Cat Male Genital Tract. *Reprod Dom Anim* **49**, 17–26. doi:10.1111/rda.12213

Arrighi S., Bosi G., Accogli G., and Desantis S. (2016). Seasonal and Ageing-Depending Changes of Aquaporins 1 and 9 Expression in the Genital Tract of Buffalo Bulls *(Bubalus bubalis)*. *Reprod Dom Anim* **51**, 515–523. doi:10.1111/rda.12713

Badran H. H., and Hermo L. S. (2002). Expression and regulation of aquaporins 1, 8, and 9 in the testis, efferent ducts, and epididymis of adult rats and during postnatal development. *J Androl* **23**, 358–373.

Barrachina F., Battistone M. A., Castillo J., Mallofré C., Jodar M., Breton S., and Oliva R. (2022). Sperm acquire epididymis-derived proteins through epididymosomes. *Human Reproduction* **37**, 651–668. doi:10.1093/humrep/deac015

Battistone M. A., Spallanzani R. G., Mendelsohn A. C., Capen D., Nair A. V., Brown D., and Breton S. (2019). Novel role of proton-secreting epithelial cells in sperm maturation and mucosal immunity (A-M Lennon-Duménil, Ed.). *Journal of Cell Science* **133**, jcs233239. doi:10.1242/jcs.233239

Campbell R., Dott H., and Glover T. (1956). Nigrosin eosin as a stain for differentiating live and dead spermatozoa. *The Journal of Agricultural Science* **48**, 1–8.

Candenas L., and Chianese R. (2020). Exosome Composition and Seminal Plasma Proteome: A Promising Source of Biomarkers of Male Infertility. *IJMS* **21**, 7022. doi:10.3390/ijms21197022

Castro M. M., Gonçalves W. G., Teixeira S. A. M. V., Fialho M. do C. Q., Santos F. C., Oliveira J. M., Serrão J. E., and Machado-Neves M. (2017). Ultrastructure and morphometric features of epididymal epithelium in Desmodus rotundus. *Micron* **102**, 35–43. doi:10.1016/j.micron.2017.08.006

Castro M. M., Kim B., Hill E., Fialho M. C. Q., Puga L. C. H. P., Freitas M. B., Breton S., and Machado-Neves M. (2017). The expression patterns of aquaporin 9, vacuolar H+-ATPase, and cytokeratin 5 in the epididymis of the common vampire bat. *Histochem Cell Biol* **147**, 39–48. doi:10.1007/s00418-016-1477-9

Chen H., Alves M. B. R., and Belleannée C. (2022). Contribution of epididymal epithelial cell functions to sperm epigenetic changes and the health of progeny. *Human Reproduction Update* **28**, 51–66. doi:10.1093/humupd/dmab029

Chen Q., and Duan E. (2011). Aquaporins in sperm osmoadaptation: an emerging role for volume regulation. *Acta Pharmacol Sin* **32**, 721–724. doi:10.1038/aps.2011.35

Cheng Q., Ding H., Fang J., Fang X., Liu H., Wang J., Chen C., and Zhang W. (2021). Aquaporin 9 Represents a Novel Target of Chronic Liver Injury That May Antagonize Its Progression by Reducing Lipotoxicity (P Muriel, Ed.). *Oxidative Medicine and Cellular Longevity* **2021**, 1–18. doi:10.1155/2021/5653700

Chung S., Kim S., Son M., Kim M., Koh E. S., Shin S. J., Ko S.-H., and Kim H.-S. (2019). Empagliflozin Contributes to Polyuria via Regulation of Sodium Transporters

583 and Water Channels in Diabetic Rat Kidneys. *Front. Physiol.* **10**, 271.
584 doi:10.3389/fphys.2019.00271

585 Clarke-Bland C. E., Bill R. M., and Devitt A. (2022). Emerging roles for AQP in
586 mammalian extracellular vesicles. *Biochimica et Biophysica Acta (BBA) -*
587 *Biomembranes* **1864**, 183826. doi:10.1016/j.bbamem.2021.183826

588 Cooper T. G., and Brooks D. E. (1981). Entry of glycerol into the rat epididymis and its
589 utilization by epididymal spermatozoa. *Reproduction* **61**, 163–169.
590 doi:10.1530/jrf.0.0610163

591 Cornwall G. A. (2009). New insights into epididymal biology and function. *Human*
592 *Reproduction Update* **15**, 213–227. doi:10.1093/humupd/dmn055

593 Da Silva N., Silberstein C., Beaulieu V., Piétrement C., Van Hoek A. N., Brown D., and
594 Breton S. (2006). Postnatal Expression of Aquaporins in Epithelial Cells of the Rat
595 Epididymis. *Biology of Reproduction* **74**, 427–438. doi:10.1095/biolreprod.105.044735

596 Delgado-Bermúdez A., Ribas-Maynou J., and Yeste M. (2022). Relevance of
597 Aquaporins for Gamete Function and Cryopreservation. *Animals* **12**, 573.
598 doi:10.3390/ani12050573

599 Domeniconi R. F., Orsi A. M., Justulin L. A., Leme Beu C. C., and Felisbino S. L.
600 (2008). Immunolocalization of aquaporins 1, 2 and 7 in rete testis, efferent ducts,
601 epididymis and vas deferens of adult dog. *Cell Tissue Res* **332**, 329–335.
602 doi:10.1007/s00441-008-0592-x

603 Feldman A. T., and Wolfe D. (2014). Tissue Processing and Hematoxylin and Eosin
604 Staining. 'Histopathology'. (Ed CE Day) Methods in Molecular Biology. pp. 31–43.
605 (Springer New York: New York, NY) doi:10.1007/978-1-4939-1050-2_3

606 Flickinger C. J., Bush L. A., Howards S. S., and Herr J. C. (1997). Distribution of
607 leukocytes in the epithelium and interstitium of four regions of the Lewis rat epididymis.
608 *Anat Rec* **248**, 380–390. doi:10.1002/(SICI)1097-0185(199707)248:3<380::AID-
609 AR11>3.0.CO;2-L

610 García-Álvarez O., Maroto-Morales A., Martínez-Pastor F., Garde J. J., Ramón M.,
611 Fernández-Santos M. R., Esteso M. C., Pérez-Guzmán M. D., and Soler A. J. (2009).
612 Sperm characteristics and in vitro fertilization ability of thawed spermatozoa from Black
613 Manchega ram: Electroejaculation and postmortem collection. *Theriogenology* **72**,
614 160–168. doi:10.1016/j.theriogenology.2009.02.002

615 Goyal H. O., and Williams C. S. (1991). Regional differences in the morphology of the
616 goat epididymis: A light microscopic and ultrastructural study. *Am. J. Anat.* **190**, 349–
617 369. doi:10.1002/aja.1001900404

618 Hermo L., Krzeczunowicz D., and Ruz R. (2004). Cell Specificity of Aquaporins 0, 3,
619 and 10 Expressed in the Testis, Efferent Ducts, and Epididymis of Adult Rats. *Journal*
620 *of Andrology* **25**, 494–505. doi:10.1002/j.1939-4640.2004.tb02820.x

621 Hermo L., Schellenberg M., Liu L. Y., Dayanandan B., Zhang T., Mandato C. A., and
622 Smith C. E. (2008). Membrane Domain Specificity in the Spatial Distribution of
623 Aquaporins 5, 7, 9, and 11 in Efferent Ducts and Epididymis of Rats. *J Histochem*
624 *Cytochem.* **56**, 1121–1135. doi:10.1369/jhc.2008.951947

Hsu S. M., and Raine L. (1981). Protein A, avidin, and biotin in immunohistochemistry. *J Histochem Cytochem.* **29**, 1349–1353. doi:10.1177/29.11.6172466

Jeyendran R. S., Van der Ven H. H., Perez-Pelaez M., Crabo B. G., and Zaneveld L. J. D. (1984). Development of an assay to assess the functional integrity of the human sperm membrane and its relationship to other semen characteristics. *Reproduction* **70**, 219–228. doi:10.1530/jrf.0.0700219

Klein C., Troedsson M. H. T., and Rutllant J. (2013). Region-Specific Expression of Aquaporin Subtypes in Equine Testis, Epididymis, and Ductus Deferens: AQP Subtypes in Stallion Reproductive Tract. *Anat. Rec.* **296**, 1115–1126. doi:10.1002/ar.22709

Li H., Kamiie J., Morishita Y., Yoshida Y., Yaoita E., Ishibashi K., and Yamamoto T. (2005). Expression and localization of two isoforms of AQP10 in human small intestine. *Biology of the Cell* **97**, 823–829. doi:10.1042/BC20040091

Marengo S. R., and Amann R. P. (1990). Morphological Features of Principal Cells in the Ovine Epididymis: A Quantitative and Qualitative Study. *Biology of Reproduction* **42**, 167–179. doi:10.1095/biolreprod42.1.167

Martínez-Fresneda L., Castaño C., Bóveda P., Tesfaye D., Schellander K., Santiago-Moreno J., and García-Vázquez F. A. (2019). Epididymal and ejaculated sperm differ on their response to the cryopreservation and capacitation processes in mouflon (Ovis musimon). *Sci Rep* **9**, 15659. doi:10.1038/s41598-019-52057-0

Martínez-Fresneda L., Sylvester M., Shakeri F., Bunes A., Del Pozo J. C., García-Vázquez F. A., Neuhoff C., Tesfaye D., Schellander K., and Santiago-Moreno J. (2021). Differential proteome between ejaculate and epididymal sperm represents a key factor for sperm freezability in wild small ruminants. *Cryobiology* **99**, 64–77. doi:10.1016/j.cryobiol.2021.01.012

Menezes T. P., Hill E., de Alencar Moura A., Lobo M. D. P., Monteiro-Moreira A. C. O., Breton S., and Machado-Neves M. (2018). Pattern of protein expression in the epididymis of Oligoryzomys nigripes (Cricetidae, Sigmodontinae). *Cell Tissue Res* **372**, 135–147. doi:10.1007/s00441-017-2714-9

Mobasheri A., Wray S., and Marples D. (2005). Distribution of AQP2 and AQP3 water channels in human tissue microarrays. *J Mol Hist* **36**, 1–14. doi:10.1007/s10735-004-2633-4

Mocé E., Blanch E., Tomás C., and Graham J. (2010). Use of Cholesterol in Sperm Cryopreservation: Present Moment and Perspectives to Future: Effect of Cholesterol on Sperm Cryopreservation. *Reproduction in Domestic Animals* **45**, 57–66. doi:10.1111/j.1439-0531.2010.01635.x

Nicander L. (1958). Studies on the regional histology and cytochemistry of the ductus epididymidis in stallions, rams and bulls. *Acta Morphol Neerl Scand* **1**, 337–362.

Nilsson L., Madsen K., Topcu S. O., Jensen B. L., Frøkiær J., and Nørregaard R. (2012). Disruption of cyclooxygenase-2 prevents downregulation of cortical AQP2 and AQP3 in response to bilateral ureteral obstruction in the mouse. *American Journal of Physiology-Renal Physiology* **302**, F1430–F1439. doi:10.1152/ajprenal.00682.2011

667 Oberska P., and Michałek K. (2021). Aquaporins: New markers for male (in)fertility in
668 livestock and poultry? *Animal Reproduction Science* **231**, 106807.
669 doi:10.1016/j.anireprosci.2021.106807

670 O'Brien E., Esteso M. C., Castaño C., Toledano-Díaz A., Bóveda P., Martínez-
671 Fresneda L., López-Sebastián A., Martínez-Nevado E., Guerra R., López Fernández
672 M., Vega R. S., Guillamón F. G., and Santiago-Moreno J. (2019). Effectiveness of ultra-
673 rapid cryopreservation of sperm from endangered species, examined by morphometric
674 means. *Theriogenology* **129**, 160–167. doi:10.1016/j.theriogenology.2019.02.024

675 Oliveira R. L., Campolina-Silva G. H., Nogueira J. C., Mahecha G. A. B., and Oliveira
676 C. A. (2013). Differential expression and seasonal variation on aquaporins 1 and 9 in
677 the male genital system of big fruit-eating bat Artibeus lituratus. *General and*
678 *Comparative Endocrinology* **186**, 116–125. doi:10.1016/j.ygcen.2013.02.041

679 Ozkocer S. E., and Konac E. (2021). The current perspective on genetic and epigenetic
680 factors in sperm maturation in the epididymis. *Andrologia* **53**,. doi:10.1111/and.13989

681 Pastor-Soler N., Bagnis C., Sabolic I., Tyszkowski R., McKee M., Van Hoek A., Breton
682 S., and Brown D. (2001). Aquaporin 9 Expression along the Male Reproductive Tract.
683 *Biology of Reproduction* **65**, 384–393. doi:10.1095/biolreprod65.2.384

684 Pequeño B., Castaño C., Alvarez-Rodriguez M., Bóveda P., Millán De La Blanca M. G.,
685 Toledano-Díaz A., Galarza D. A., Rodriguez-Martinez H., Martínez-Madrid B., and
686 Santiago-Moreno J. (2023). Variation of existence and location of aquaporin 3 in
687 relation to cryoresistance of ram spermatozoa. *Front. Vet. Sci.* **10**, 1167832.
688 doi:10.3389/fvets.2023.1167832

689 Pequeño B., Martínez-Madrid B., Castaño C., Toledano-Díaz A., Bóveda P., Esteso M.
690 C., Gómez-Guillamón F., Prieto P., Marcos-Beltrán J. L., Alvarez-Rodriguez M.,
691 Rodriguez-Martinez H., and Santiago-Moreno J. (2023). Location of aquaporins 3, 7
692 and 10 in frozen-thawed ejaculated and cauda epididymal spermatozoa from the
693 Iberian ibex, mouflon, and chamois. *Theriogenology Wild* **2**, 100025.
694 doi:10.1016/j.therwi.2023.100025

695 Pradiee J., O'Brien E., Esteso M. C., Castaño C., Toledano-Díaz A., Lopez-Sebastián
696 A., Marcos-Beltrán J. L., Vega R. S., Guillamón F. G., Martínez-Nevado E., Guerra R.,
697 and Santiago-Moreno J. (2016). Effect of shortening the prefreezing equilibration time
698 with glycerol on the quality of chamois (Rupicapra pyrenaica), ibex (Capra pyrenaica),
699 mouflon (Ovis musimon) and aoudad (Ammotragus lervia) ejaculates. *Animal*
700 *Reproduction Science* **171**, 121–128. doi:10.1016/j.anireprosci.2016.06.007

701 Pursel V. G., and Johnson L. A. (1974). Glutaraldehyde fixation of boar spermatozoa
702 for acrosome evaluation. *Theriogenology* **1**, 63–68. doi:10.1016/0093-691X(74)90008-
703 9

704 Robaire B., and Hinton B. T. (2015). The Epididymis. 'Knobil and Neill's Physiology of
705 Reproduction'. pp. 691–771. (Elsevier) doi:10.1016/B978-0-12-397175-3.00017-X

706 Santiago-Moreno J., Astorga R. J., Luque I., Coloma M. A., Toledano-Díaz A., Pulido-
707 Pastor A., Gómez-Guillamon F., Salas-Vega R., and López-Sebastián A. (2009).
708 Influence of recovery method and microbial contamination on the response to freezing–
709 thawing in ibex (Capra pyrenaica) epididymal spermatozoa. *Cryobiology* **59**, 357–362.
710 doi:10.1016/j.cryobiol.2009.09.012

Santiago-Moreno J., Pequeño B., Martinez-Madrid B., Castaño C., Bóveda P., Velázquez R., Toledano-Díaz A., Álvarez-Rodríguez M., and Rodríguez-Martínez H. (2022). Expression of Aquaglyceroporins in Spermatozoa from Wild Ruminants Is Influenced by Photoperiod and Thyroxine Concentrations. *IJMS* **23**, 2903. doi:10.3390/ijms23062903

Schimming B., Baumam C., Pinheiro P., de Matteis R., and Domeniconi R. (2017). Aquaporin 9 is expressed in the epididymis of immature and mature pigs. *Reprod Dom Anim* **52**, 617–624. doi:10.1111/rda.12957

Schimming B. C., Martins L. L., Oliveira F. S. de, Pinheiro P. F. F., and Domeniconi R. F. (2021). Morphology and immunolocalization of aquaporins 1 and 9 in the agouti (Dasyprocta azarae) testis excurrent ducts. *Anim. Reprod.* **18**, e20210070. doi:10.1590/1984-3143-ar2021-0070

Schimming B., Pinheiro P., de Matteis R., Machado C., and Domeniconi R. (2015). Immunolocalization of Aquaporins 1 and 9 in the Ram Efferent Ducts and Epididymis. *Reprod Dom Anim* **50**, 617–624. doi:10.1111/rda.12537

Serre V., and Robaire B. (1998). Segment-Specific Morphological Changes in Aging Brown Norway Rat Epididymis. *Biology of Reproduction* **58**, 497–513. doi:10.1095/biolreprod58.2.497

Serre V., and Robaire B. (1999). Distribution of Immune Cells in the Epididymis of the Aging Brown Norway Rat Is Segment-Specific and Related to the Luminal Content. *Biology of Reproduction* **61**, 705–714. doi:10.1095/biolreprod61.3.705

Squillacioti C., Mirabella N., Liguori G., Germano G., and Pelagalli A. (2021). Aquaporins Are Differentially Regulated in Canine Cryptorchid Efferent Ductules and Epididymis. *Animals* **11**, 1539. doi:10.3390/ani11061539

Sullivan R., Frenette G., and Girouard J. (2007). Epididymosomes are involved in the acquisition of new sperm proteins during epididymal transit. *Asian J Andrology* **9**, 483–491. doi:10.1111/j.1745-7262.2007.00281.x

Trasler J. M., Hermo L., and Robaire B. (1988). Morphological Changes in the Testis and Epididymis of Rats Treated with Cyclophosphamide: A Quantitative Approach. *Biology of Reproduction* **38**, 463–479. doi:10.1095/biolreprod38.2.463

Varisli O., Uguz C., Agca C., and Agca Y. (2009). Motility and acrosomal integrity comparisons between electro-ejaculated and epididymal ram sperm after exposure to a range of anisosmotic solutions, cryoprotective agents and low temperatures. *Animal Reproduction Science* **110**, 256–268. doi:10.1016/j.anireprosci.2008.01.012

Yeste M., Morató R., Rodríguez-Gil J., Bonet S., and Prieto-Martínez N. (2017). Aquaporins in the male reproductive tract and sperm: Functional implications and cryobiology. *Reprod Dom Anim* **52**, 12–27. doi:10.1111/rda.13082

749 **Table 1. Percentual determination of epithelial cell types on epididymal**
750 **caput, corpus, and cauda regions of Iberian ibex, mouflon, and chamois** (mean ±
751 SEM). For a given epithelial cell type and epididymal region, means with different
752 superscript letters (a, b, c) differ significantly (P<0.05) between species.

Epididymal region	Species	Epithelial cell types (% cell/tubule)				
		Principal	Basal	Clear	Apical	Halo
Caput	Ibex	76.0 ± 1.9 ^{b}	13.7 ± 1.8 ^{a}	2.7 ± 0.8 ^{a}	3.6 ± 0.6	4.1 ± 1.9
	Mouflon	88.0 ± 2.3 ^{a}	6.2 ± 0.4 ^{b}	0.9 ± 0.4 ^{b}	2.9 ± 0.7	2.0 ± 0.3
	Chamois	81.8 ± 1.2 ^{a}	9.5 ± 0.9 ^{ab}	1.7 ± 0.9 ^{ab}	3.9 ± 0.6	3.1 ± 0.9
Corpus	Ibex	61.5 ± 1.4 ^{b}	28.1 ± 1.2 ^{a}	4.2 ± 0.3 ^{a}	2.7 ± 0.3 ^{b}	3.5 ± 0.7
	Mouflon	78.1 ± 1.6 ^{a}	11.4 ± 0.9 ^{b}	1.5 ± 0.1 ^{c}	5.3 ± 0.6 ^{a}	3.7 ± 0.2
	Chamois	75.0 ± 2.7 ^{a}	12.8 ± 0.5 ^{b}	2.7 ± 0.3 ^{b}	4.8 ± 0.5 ^{a}	4.7 ± 0.4
Cauda	Ibex	70.3 ± 1.5 ^{b}	18.3 ± 2.1	3.7 ± 0.3 ^{ab}	2.5 ± 0.4	5.1 ± 0.9
	Mouflon	79.6 ± 3.5 ^{a}	11.9 ± 1.6	3.5 ± 0.5 ^{b}	2.26 ± 0.8	2.8 ± 0.7
	Chamois	78.2 ± 1.4 ^{ab}	11.1 ± 1.4	5.3 ± 0.4 ^{a}	1.3 ± 0.3	4.0 ± 0.2

753

754

Table 2. Main aquaporin 3, 7, 9, and 10 immunoexpression membrane patterns in the epithelial cell types of epididymal caput, corpus, and cauda regions of Iberian ibex, mouflon, and chamois. Principal: principal cells; Apical: apical cells; Basal: basal cells; m: membrane; am: apical membrane; bm: basal membrane; -, not immunoreactivity.

Epididymal region	AQPs	Species		
		Iberian ibex	Mouflon	Chamois
Caput	AQP3	Basal (m, sporadic)	Basal (m, sporadic)	Basal (m, sporadic)
	AQP7	Principal (m, weak) Basal (m)	Principal (m, weak) Apical (am, sporadic)	Principal (m, weak) Apical (am, sporadic)
	AQP9	Principal (am, bm) Apical (am) Basal (m)	Principal (am, bm) Apical (am) Basal (m)	Principal (am, bm) Apical (am) Basal (m)
	AQP10	-	-	-
Corpus	AQP3	Principal (am) Apical (am)	Principal (am) Apical (am)	Principal (am) Apical (am)
	AQP7	Basal (m, weak)	Basal (m, weak)	Basal (m, weak)
	AQP9	Principal (am, bm) Apical (am) Basal (m)	Principal (am, bm) Apical (am) Basal (m)	Principal (am, bm) Apical (am) Basal (m)
	AQP10	-	Principal (am) Apical (am) Basal (m)	Principal (am, weak) Apical (am, weak) Basal (m)
Cauda	AQP3	Basal (m, sporadic)	Basal (m, sporadic)	Basal (m, sporadic)
	AQP7	Principal (am)	Principal (am, sporadic)	-
	AQP9	Principal (am) Apical (am)	Principal (am) Apical (am)	Principal (am) Apical (am)
	AQP10	Principal (am) Basal (m)	Basal (m)	Basal (m)

Table 3. Effect of species on quality sperm variables in fresh and frozen-thawed epididymal samples (mean ± SEM). Means with different capital letter superscripts differ significantly (P<0.05) between species in fresh samples; means with different lowercase letter superscripts differ significantly (P<0.05) between species in frozen-thawed samples.

Sperm variables	Fresh epididymal samples			Frozen-thawed epididymal samples		
	Ibex	Mouflon	Chamois	Ibex	Mouflon	Chamois
Concentration (x10^6 mL^{-1})	2224.0 ± 407.7 ^{B}	5688.0 ± 789.8 ^{A}	5688.0 ± 789.8 ^{A}	- -	- -	- -
Viability (%)	77.4 ± 5.8	89.6 ± 2.0	88.0 ± 4.5	62,4 ± 9 ^{ab}	53 ± 5,4 ^{b}	70,3 ± 4,5 ^{a}
Membrane functional integrity (HOST) (%)	94.6 ± 1.5 ^{A}	92.1 ± 2.2 ^{AB}	88.2 ± 1.8 ^{B}	74,8 ± 3,9 ^{a}	59,6 ± 2,1 ^{b}	62,8 ± 6,7 ^{ab}
Intact acrosome (%)	97.5 ± 1.2	96.4 ± 1.3	96.2 ± 0.6	69,4 ± 10,8	58,6 ± 7,8	73,6 ± 3,7
Morphological abnormalities (%)	3.2 ± 1.3	3.7 ± 0.6	2.5 ± 0.3	21,8 ± 7,3	17,2 ± 7,1	16,8 ± 4,3
Total sperm motility (%)	84.0 ± 3.0	95.0 ± 0.3	73.3 ± 7.3	-	-	-
Quality of motility (0-5)	3.2 ± 0.38 ^{AB}	4.2 ± 0.17 ^{A}	2.3 ± 0.25 ^{B}	-	-	-
Total sperm motility (TM) (%)	-	-	-	55,9 ± 11,4	38,19 ± 9,45	42,2 ± 6,4
Progressive motility (pm) (%)	-	-	-	37,7 ± 9,3	33,5 ± 9,47	12,7 ± 3,9
Curvilinear velocity (VCL) (µm/s)	-	-	-	95,5 ± 9,2 ^{ab}	121,28 ± 8,96 ^{a}	55,7 ± 10,2 ^{b}
Straight line velocity (VSL) (µm/s)	-	-	-	39,4 ± 3,5 ^{b}	64,9 ± 10,4 ^{a}	22,5 ± 2,5 ^{c}
Average path velocity (VAP) (µm/s)	-	-	-	53,5 ± 4,3 ^{b}	83,7 ± 11,1 ^{a}	33,8 ± 4,9 ^{c}
Amplitude of lateral head (ALH) (µm)	-	-	-	4,0 ± 0,4	4,18 ± 0,26	2,5 ± 0,4

Table S1. Inmunolabeling of AQP3, AQP7, AQP9, and AQP10 in the apical blebs of Iberian ibex, mouflon, and chamois epididymal epithelium.

Epididymal region	Species	AQP3	AQP7	AQP9	AQP10
Caput	Ibex	-	+	+	+
	Mouflon	-	+	+	+
	Chamois	+	+	+	+
Corpus	Ibex	+	+	+	+
	Mouflon	+	+	+	+
	Chamois	+	+	+	+
Cauda	Ibex	-	+	+	-
	Mouflon	-	+	+	-
	Chamois	-	+	+	-

770 **FIGURE LEGENDS**

771

772 **Fig. 1. Iberian ibex epididymis in caput, corpus, and cauda regions.** *(a)*
773 Caput region. *(b)* Corpus region. *(c)* Cauda region. Principal (p), basal (b), apical (a),
774 clear (c), and halo (h) cells appear in the epithelium lining, which lies on the periductal
775 stroma (st). Note stereocilia (sc) and spermatozoa (*) in the tubular lumen (Lumen).
776 Haematoxylin and eosin stain, 400X. Bar = 50 µm.

777

778

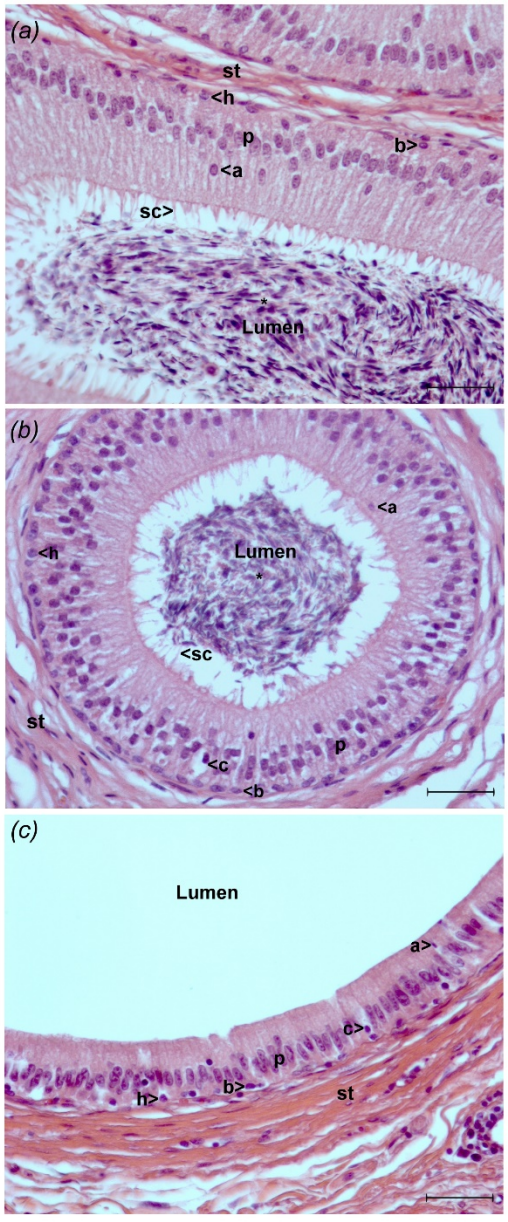

780 **Fig. 2. Mouflon epididymis in caput, corpus, and cauda regions.** *(a)* Caput
781 region. *(b)* Corpus region. *(c)* Cauda region. Principal (p), basal (b), clear (c), apical (a),
782 and halo (h) cells appear in the epithelium lining, which lies on the periductal stroma (st).
783 Note stereocilia (sc) and spermatozoa (*) in the tubular lumen (Lumen). Haematoxylin
784 and eosin stain, 400X. Bar = 50 µm.

785

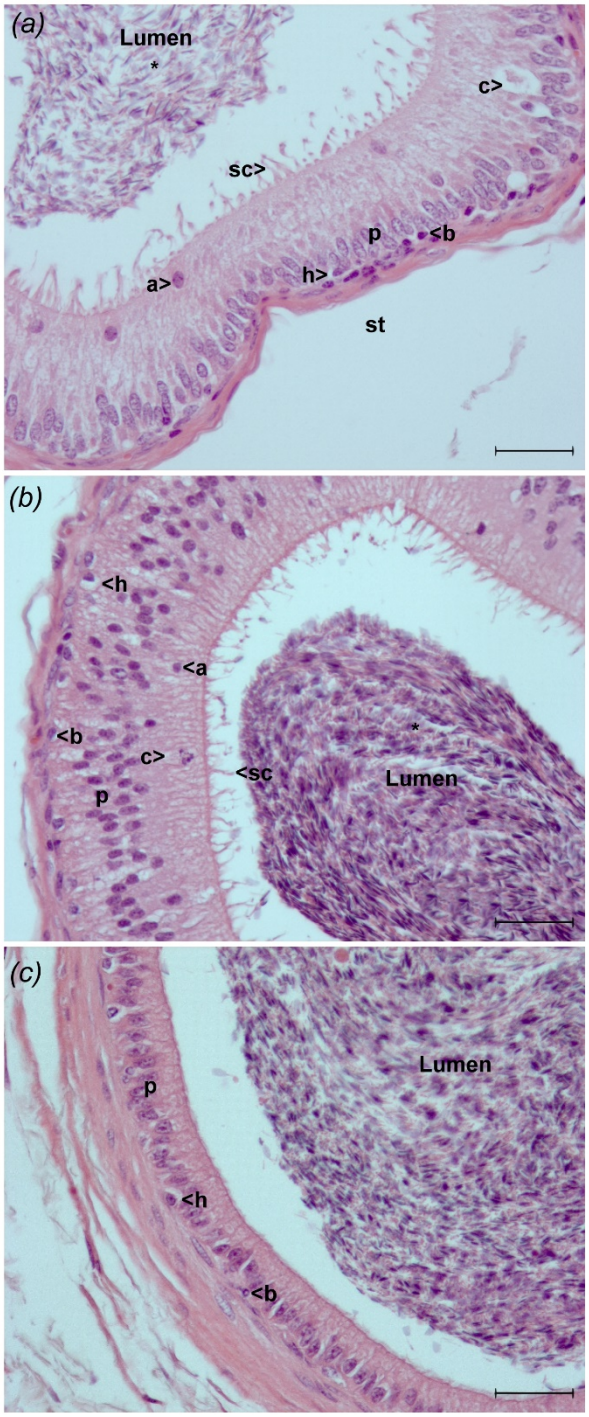

786

787

788 **Fig. 3. Chamois epididymis in caput, corpus, and cauda regions.** *(a)* Caput
789 region. *(b)* Corpus region. *(c)* Cauda region. Principal (p), basal (b), clear (c), apical (a),
790 and halo (h) cells appear in the epithelium lining, which lies on the periductal stroma (st).
791 Note stereocilia (sc) and spermatozoa (*) in the tubular lumen (Lumen). Haematoxylin
792 and eosin stain, 400X. Bar = 50 µm.

793

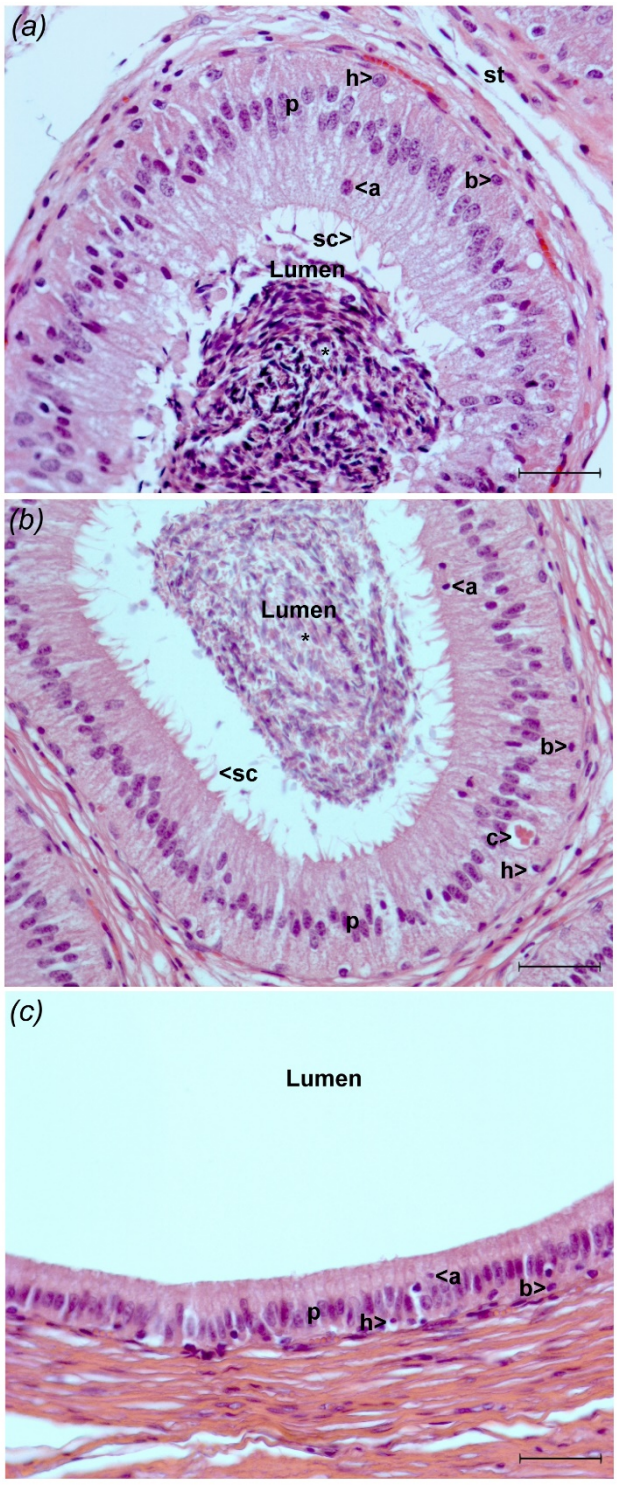

794

795

796 **Fig. 4. Immunolabeling of T-CD3 antigen on halo cells in caput, corpus, and cauda**
797 **region of Iberian ibex, mouflon, and chamois epididymis.** Overview of distribution of
798 T-CD3^{+} cells within the tubules *(a-c, g-i, m-o)* (400X), and detail at higher magnification
799 *(d-f, j-l, p-r)*. Bar = 50 µm.

800

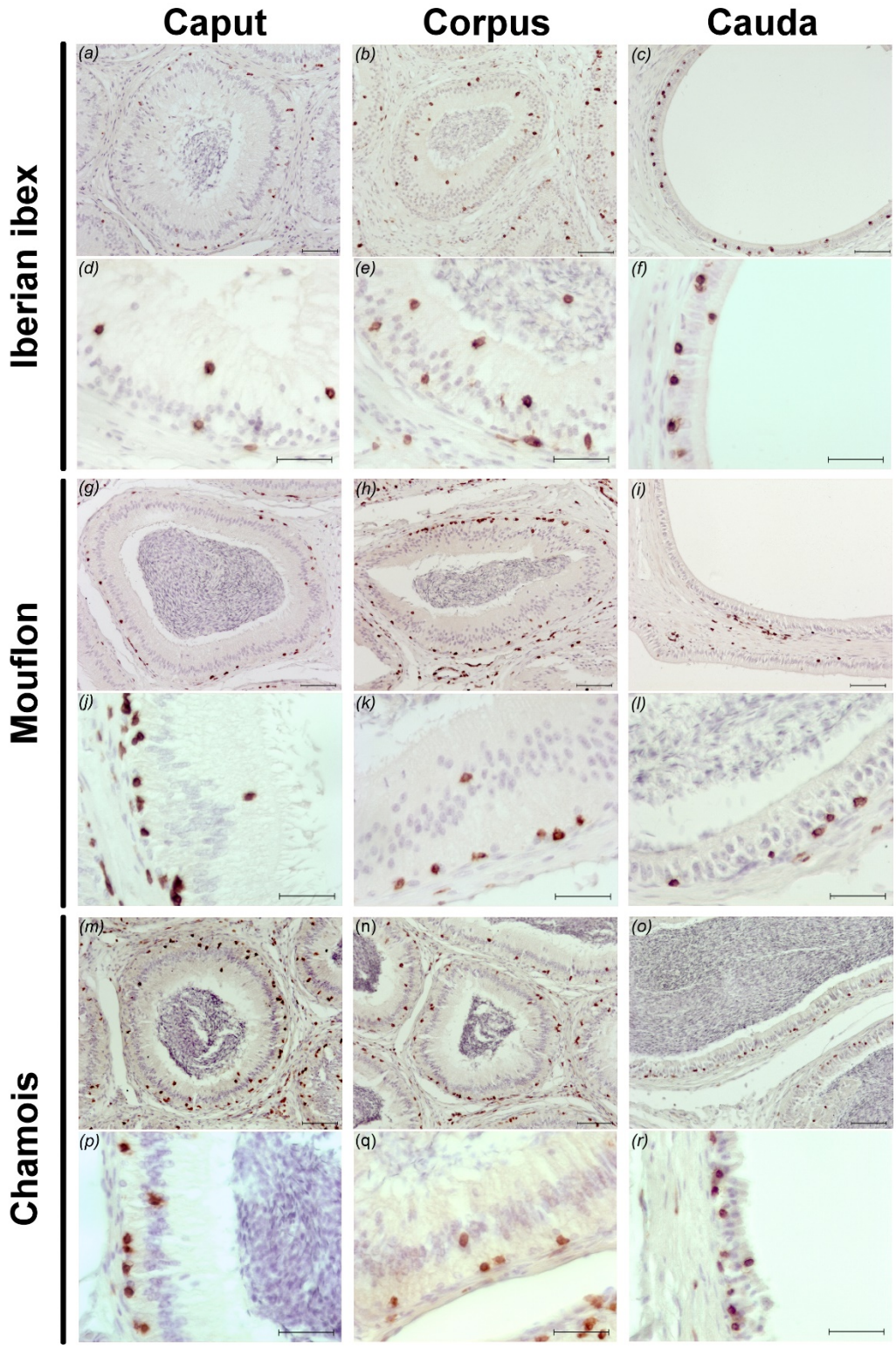

801

Fig. 5. Effect of species on epithelial epididymis cell type percentages (means ± SEM). For a given epithelial cell type, means joined by a horizontal bar differ significantly (P<0.05) between species.

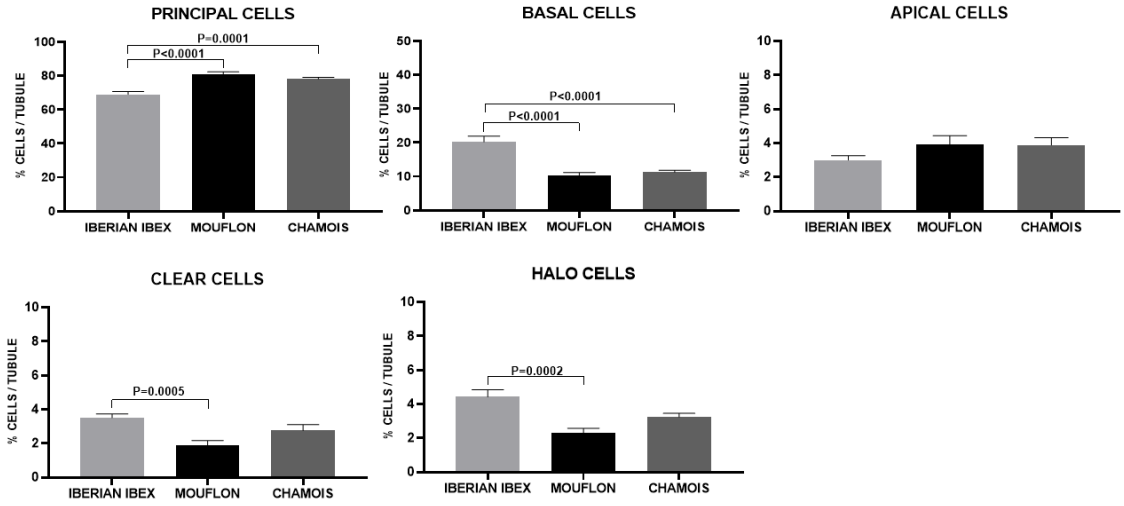

Fig. 6. Aquaporin 3, 7, 9, and 10 immunohistochemistry in caput region of Iberian ibex, mouflon, and chamois epididymis. 400X. Bar = 50 µm.

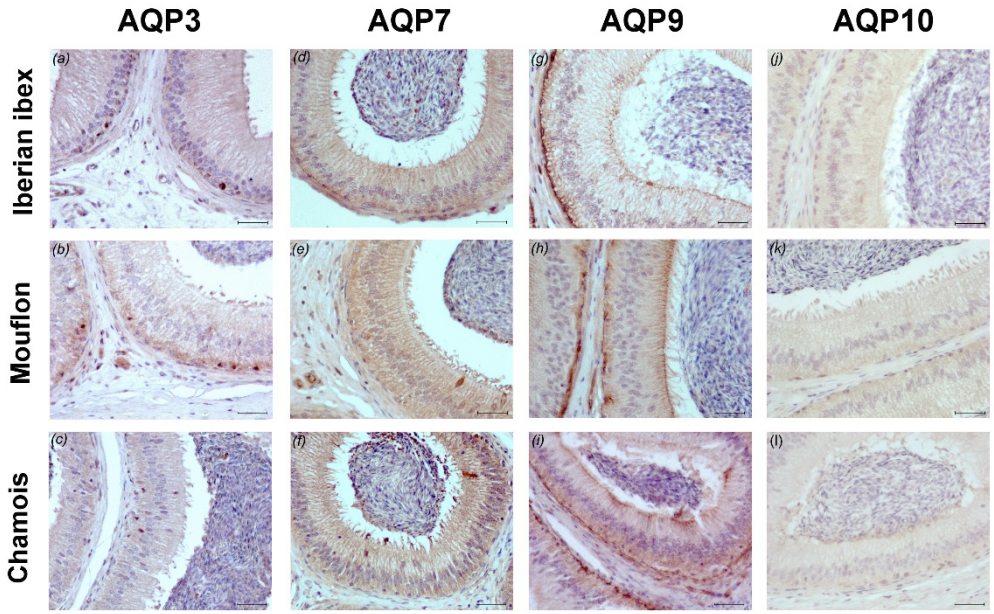

Fig. 7. Aquaporin 3, 7, 9, and 10 immunohistochemistry in corpus region of Iberian ibex, mouflon, and chamois epididymis. 400X. Bar = 50 µm.

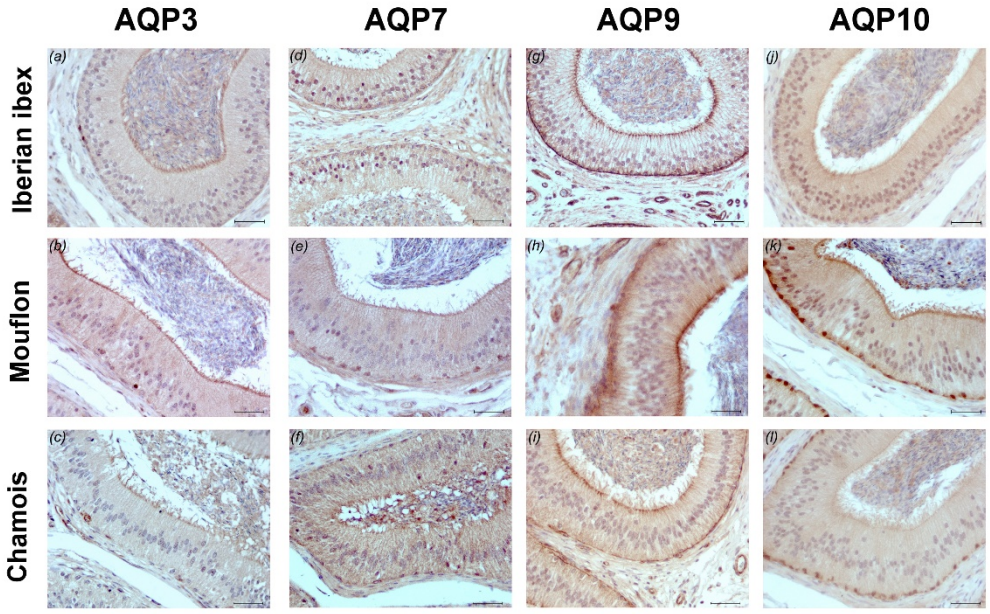

Fig. 8. Aquaporin 3, 7, 9, and 10 immunohistochemistry in cauda region of Iberian ibex, mouflon, and chamois epididymis. 400X. Bar = 50 µm.

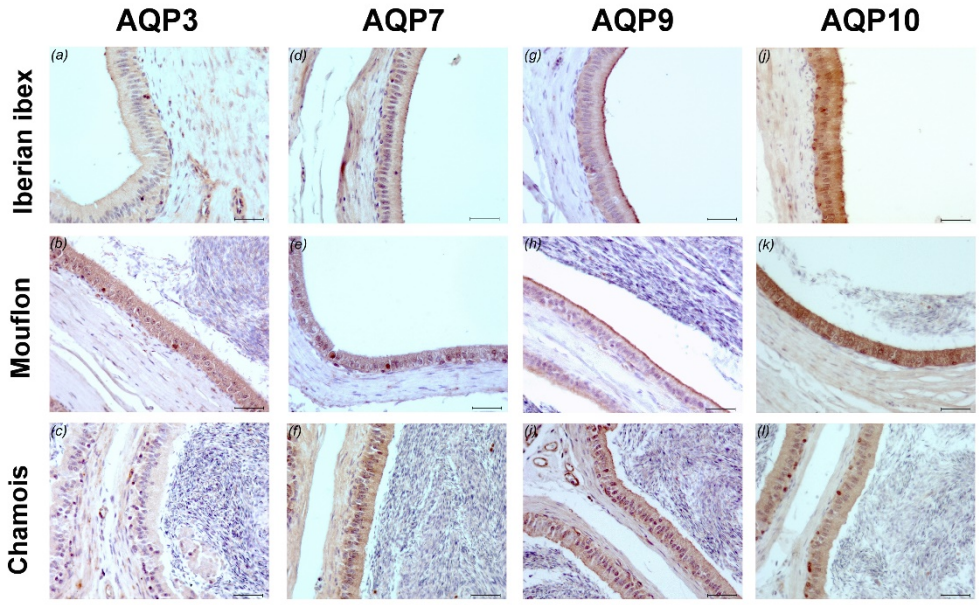

Fig. S1. Positive controls for aquaporin 3, 7, 9, and 10 immunohistochemistry. *(a)* Mouse kidney (for AQP3). *(b)* Rat kidney (for AQP7). *(c)* Rat liver (for AQP9). *(d)* Human yeyune (for AQP10). 400X. Bar = 50 μm.

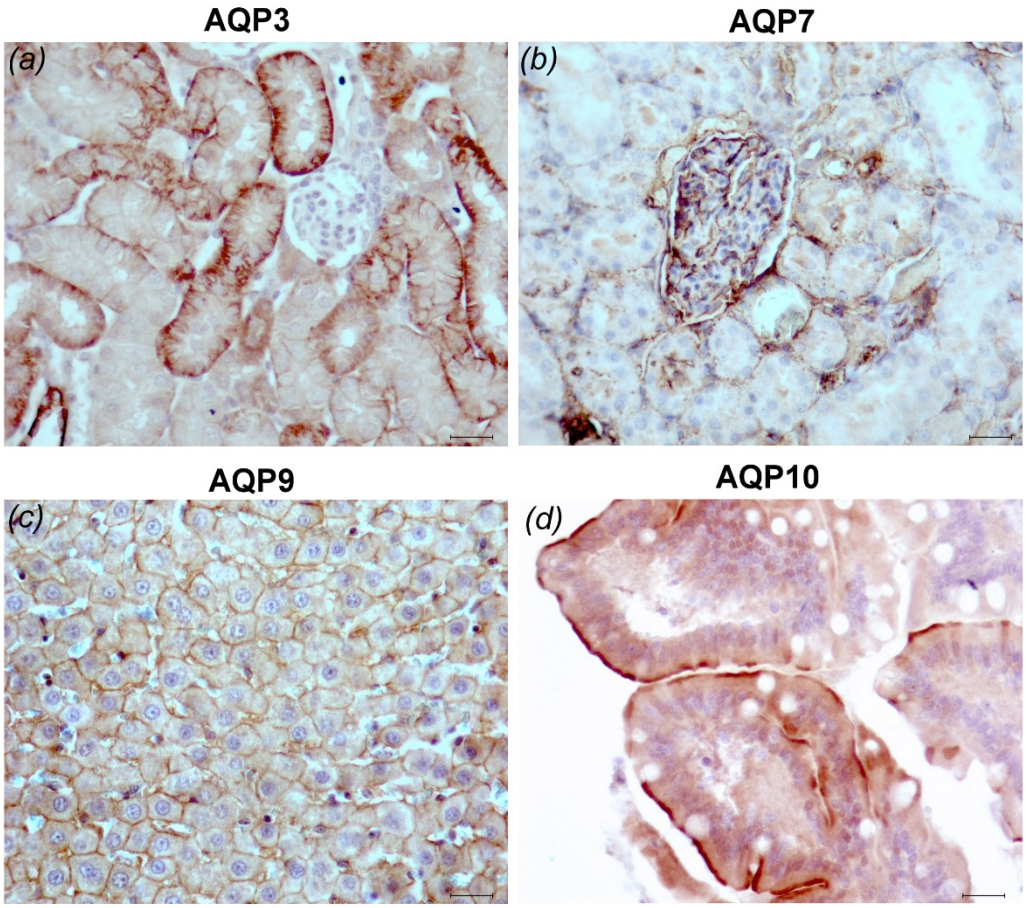

Fig. S2. Negative controls for aquaporin 3, 7, 9, and 10 immunohistochemistry of Iberian ibex, mouflon, and chamois epididymis. *(a-c)* Caput, *(d-f)* corpus, *(g-i)* and cauda regions of Iberian ibex, mouflon, and chamois epididymis, respectively. 400X. Bar = 50 µm.

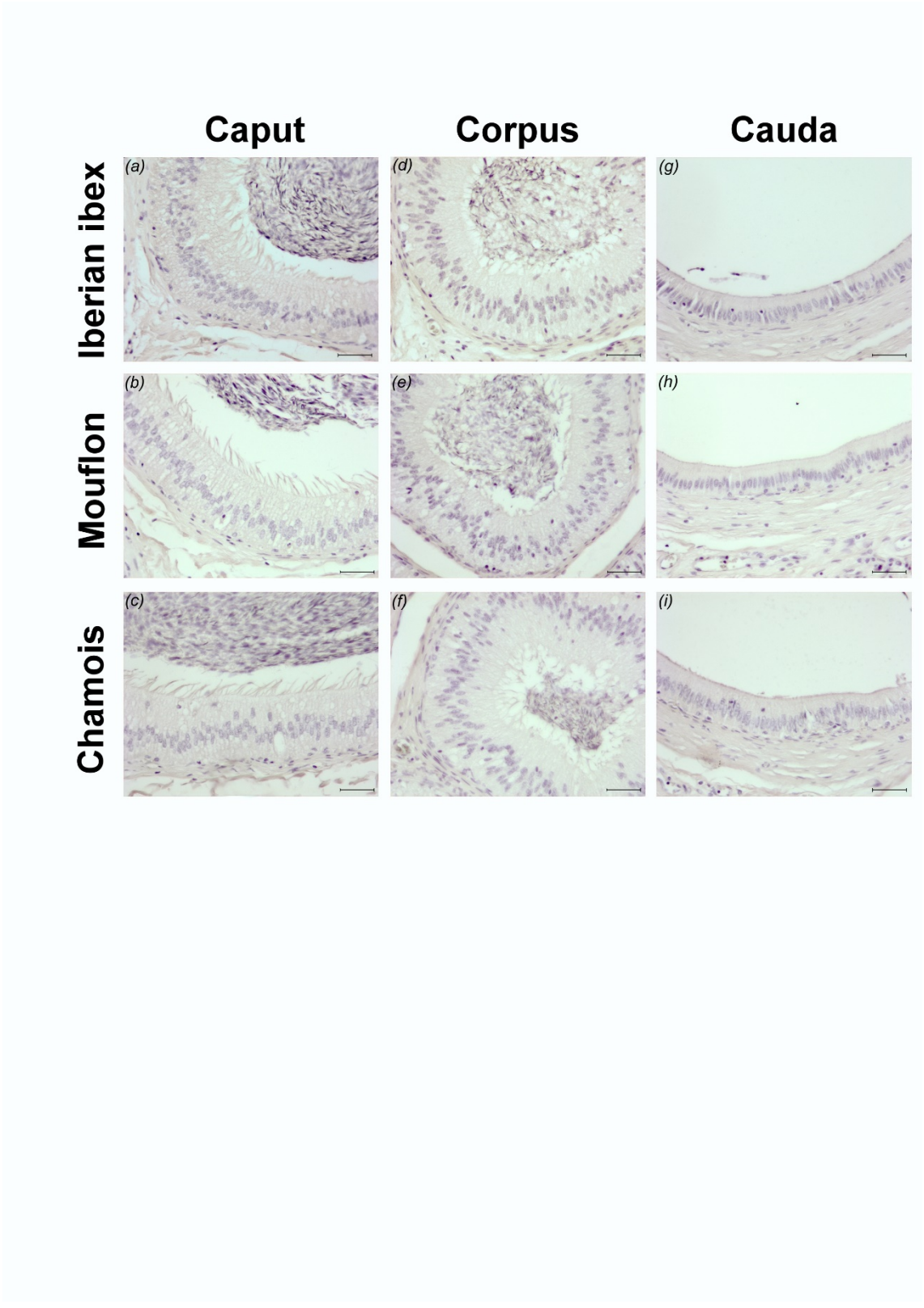

Fig. S3. Peptide-blocking experiments to test the specificity of aquaporin 3, 7, and 9 antibodies in caput, corpus, and cauda region of Iberian ibex epididymis and ovine kidney. For aquaporin 3, 7, and 9, in the upper files (a-d, i-l, q-t), the positive immunolabeling after incubating with the primary antibody, and in the lower files (e-h, m-p, u-x), the lack of immunolabeling resulting from incubation also with the respective aquaporin blocking peptide. 630X. Bar = 50 µm.

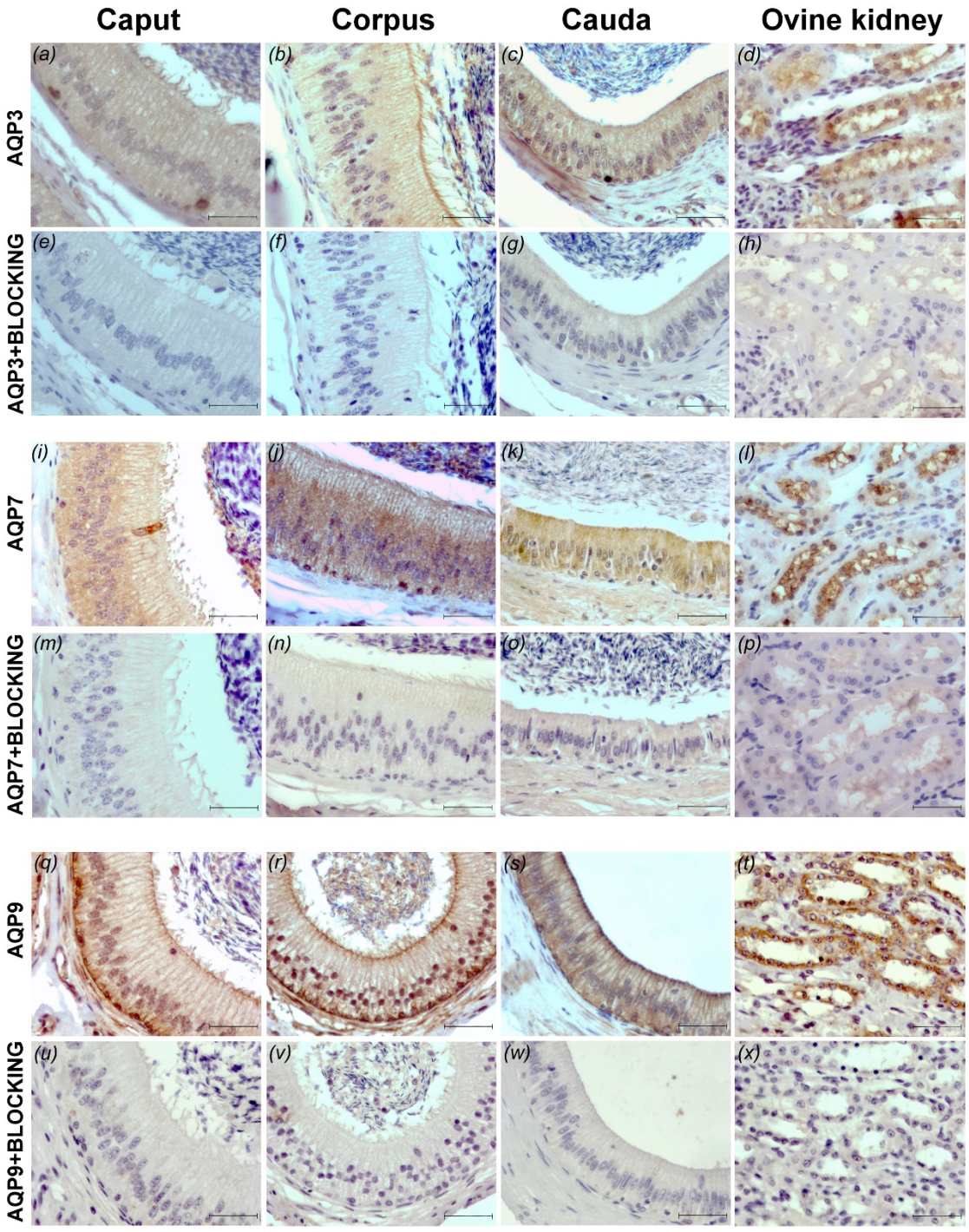

Fig. S4. Detail of aquaporin 3, 7, 9, and 10 immunolabeling in caput region of Iberian ibex, mouflon, and chamois epididymis. 630X. Bar = 50 µm.

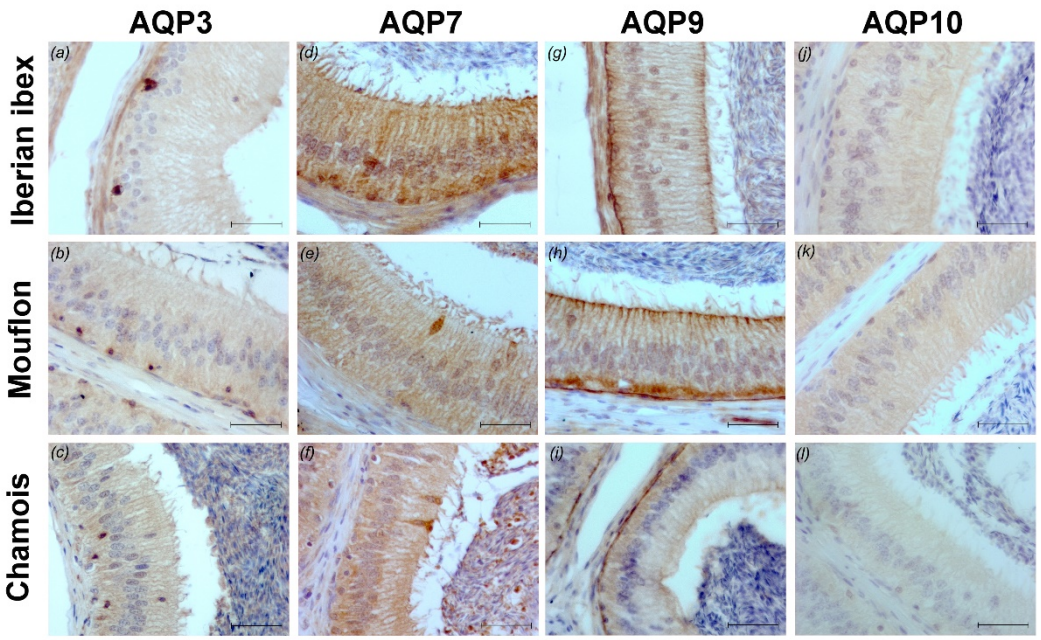

Fig. S5. Detail of aquaporin 3, 7, 9, and 10 immunolabeling in corpus region of Iberian ibex, mouflon, and chamois epididymis. 630X. Bar = 50 µm.

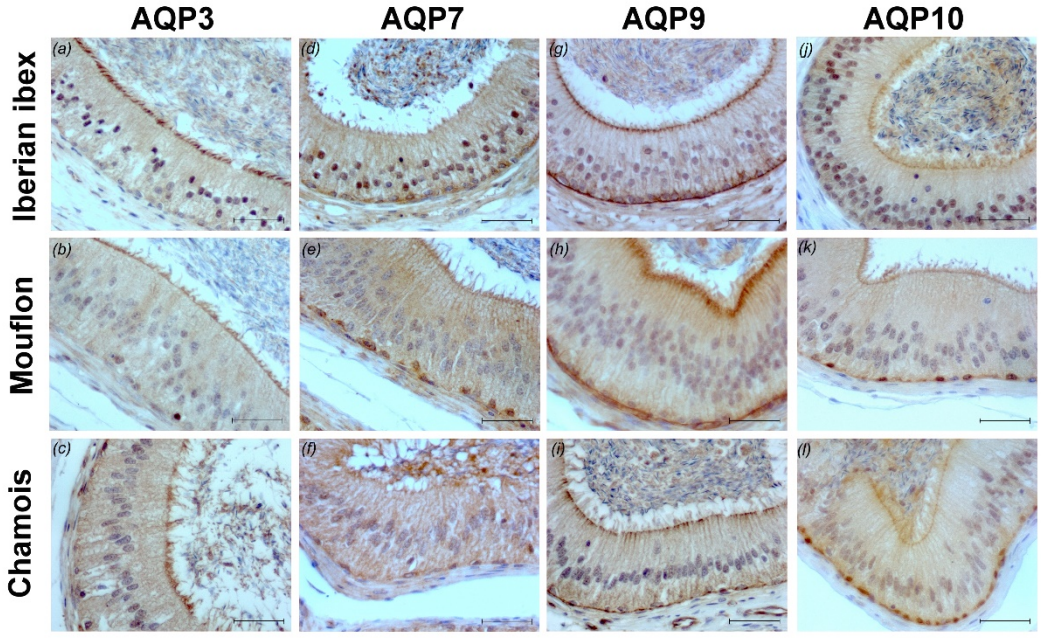

Fig. S6. Detail of aquaporin 3, 7, 9, and 10 immunolabeling in cauda region of Iberian ibex, mouflon, and chamois epididymis. 630X. Bar = 50 µm.

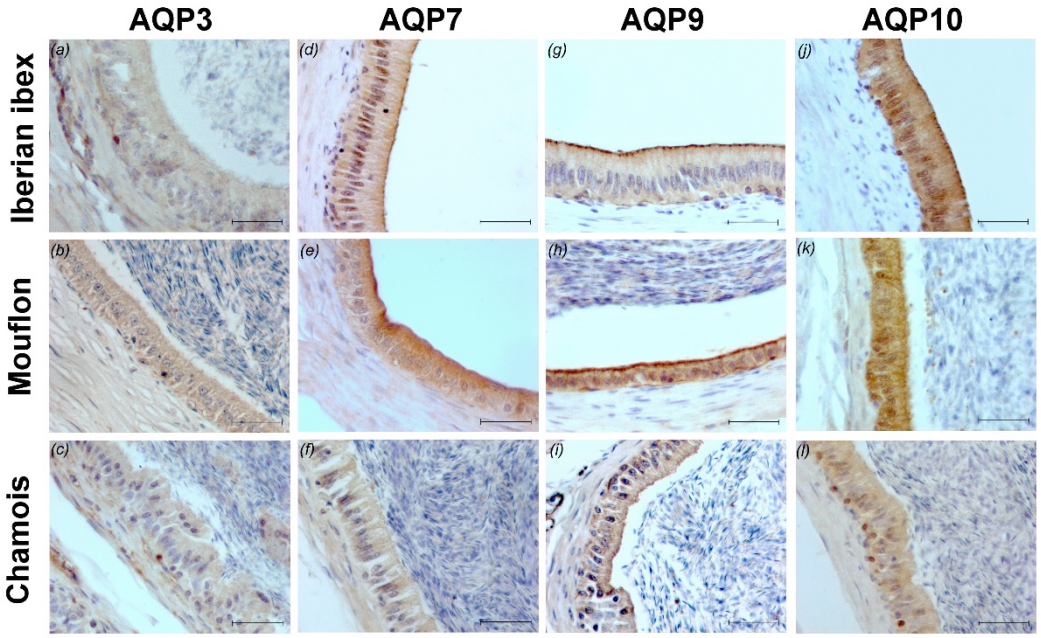

Fig. S7. Illustrative images of the apical blebs immunolabeling in the caput, corpus, and cauda regions of the epididymal epithelium. The images show the aquaporin 9 immunolabeling in the lumen of caput (a), corpus (b), and cauda (c) epididymis of Iberian ibex as a representative example for all the studied AQPs and wild ruminant species. 630X. Bar = 50 µm.